ONSHORE BURIED STEEL FUEL PIPELINES AT FAULT CROSSINGS: A REVIEW OF CRITICAL ANALYSIS AND DESIGN ASPECTS

Vasileios E. Melissianos[1]

Abstract: Onshore buried steel pipeline infrastructure is a critical component of the fuel supply system. Pipeline failure due to seismic actions is socially, environmentally, and economically unacceptable and thus the design of pipelines at geohazard areas, such as fault crossings, remains a hot topic for the pipeline community. There is an intense research effort on the evaluation of the pipeline mechanical behavior and the strength verification at fault crossings. Still, some aspects need in-depth consideration concerning practical applications. A state-of-the-art review is presented on three critical analysis and design aspects, namely the calculation of the design fault displacement via deterministic and probabilistic methods, the effect of numerical modeling parameters such as soil spring properties, and the alternative pipe protection measures in terms of availability, efficiency, and selection process. The critical review offers a thorough insight on what is available and how to employ it in design, assisting engineers and pipe operators in improving pipe safety.

[1]Research Associate, Institute of Steel Structures, School of Civil Engineering, National Technical University of Athens, 9 Iroon Polytechneiou str., Zografou Campus, GR-15780 Athens, Greece (corresponding author). E-mail: melissia@mail.ntua.gr

Author Keywords: buried pipeline; fault crossing; design fault displacement; numerical modeling; protection measures

Introduction

Onshore buried continuous steel pipelines are the essential link in the fuel supply system, interconnecting wells, storage facilities, process plants, and customers. Pipes have been proven to be the cheapest and most efficient mode of transporting oil and gas for almost 100 years (Strogen et al. 2016). Securing the integrity of pipeline networks against seismic actions with state-of-the-art tools (Fragiadakis et al. 2015) is crucial for the safety and prosperity of communities. A pipe failure could be disastrous for society, the environment, and the economy due to injuries or fatalities, air/soil/water contamination, monetary losses, and downtimes, respectively (Nair et al. 2018; Papadakis 1999). Seismic fault activation is the most catastrophic seismic-induced action on pipelines (Girgin and Krausmann 2016). The fault mechanism, namely normal, reverse, or strike-slip, is the dominant parameter affecting the pipe response because it determines the pipe deformation (Fig. 1). Pipe tension and pipe compression are predominant in cases of normal and reverse faulting, respectively while bending dominates the pipe behavior in case of strike-slip faulting (O’Rourke and Liu 2012). Modern codes (Table 1) provide recommendations and guidelines for the design and assessment of pipes at fault crossings.

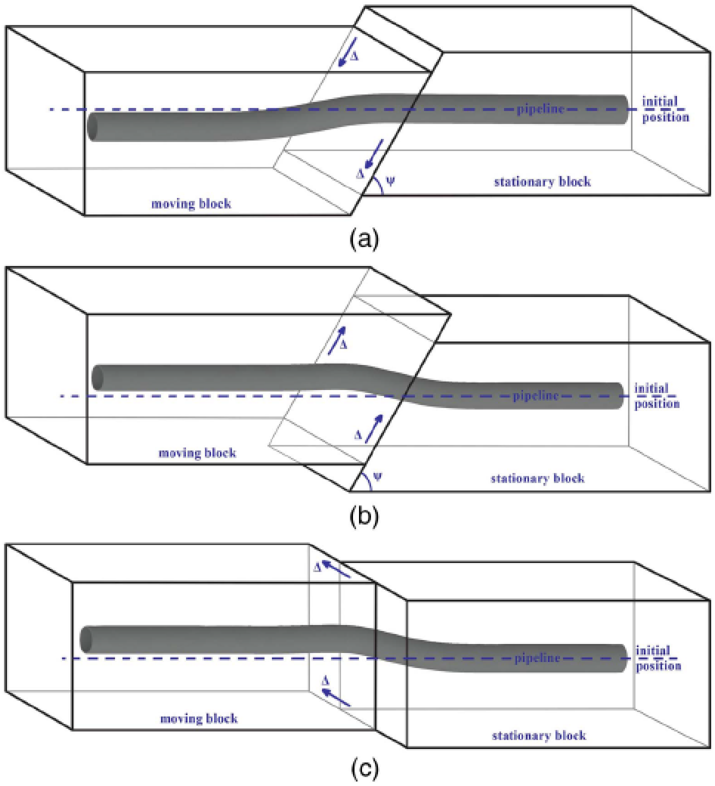

Fig. 1. Pipeline deformation caused by (a) normal; (b) reverse; and (c) strike-slip fault rupture (the left block is the moving and the right is the stationary one).

The potential failure modes of a pipeline subjected to faulting are local buckling of the pipeline wall, tensile rupture, cross-section ovalization, and beam-mode buckling in the case of reverse faulting. Strength verification of pipes under faulting (displacement-controlled loading) against local buckling and tensile fracture is carried out in strain terms. Mohr (2003) justifies the adoption of strain-based performance limits through an example: if two pipes of different steel grades are fitted to a curved ground surface, then the same strain level would be developed, unlike the stress level because strains are unambiguously defined by the ground curvature.

The compressive strain shall be limited to ensure that local buckling of the pipeline wall is avoided. The concentration of compression leads to the initiation of a wrinkle that neither interrupts fuel flow nor allows a leak. Further increase of compression allows the evolvement of the wrinkle to a local buckle, stating a limit state exceedance (Houliara and Karamanos 2006; Karamanos 2002; Kyriakides and Corona 2007). Parameters affecting the compressive strain capacity of a pipe are (1) the girth welds that might “attract” the buckle to a nearby region (Dorey et al. 2000; Prion and Birkemoe 1992), (2) the pressurization that relieves the compression as it creates tensile hoop stresses preventing cross-section distortion (Greiner and Guggenberger 1998; Limam et al. 2010), and (3) the external pressure that reduces the resistance to local buckling (Vasilikis and Karamanos 2011) and might contribute to buckling propagation (Corona and Kyriakides 1991, 2000). The seminal work of Gresnigt (1986) has contributed to the development of limiting expressions for the compressive strain.

Tensile strains may cause rupture of the pipeline wall at areas of strain concentration. Girth welds between two adjacent pipeline segments are considered to be the weak link due to the imperfections associated with the welding process (Wang et al. 2004), the reduced ductility in the heat-affected zone, the potential tolerable defects, and the potential corrosion due to coating on-site (Abdulhameed et al. 2016; O’Rourke and Liu 2012). Note that apart from the recent PRCI Guidelines that are based on the work of Liu et al. (2012a; b) and Wang et al. (2012), typically high-quality welding and a defect-free homogenous pipe material (Liu et al. 2009) is assumed in the code expressions for the tensile strain capacity.

The crossing pipeline is subjected to significant compression in the case of reverse faulting, leading to potential pipe local or global buckling. The latter is denoted also as upheaval buckling or beam-mode buckling and is typically defined as the exposure of the pipe on the ground surface (Demirci et al. 2018; Rofooei et al. 2018; Rojhani et al. 2012). Pipe global buckling caused by fault movement has been reported by Koch (1933) at the Buena Vista Hills Oil Filed in California, USA, and by Hamada and O’Rourke (1992) after the 1964 Niigata, Japan earthquake. Global buckling might not result in a failure but local buckling might follow shortly after (Liu et al. 2017; Xu and Lin 2017). Whether the pipe will buckle locally on globally depends on the local slenderness (diameter to thickness ratio D/t) and the burial depth. Deeply buried pipes with a high D/t ratio tend to buckle locally, while shallowly buried ones with low D/t ratio tend to buckle globally (Melissianos et al. 2020; Yun and Kyriakides 1990). Specific guidelines for the assessment and protection of pipes against global buckling are not provided in design codes, apart from the general requirement of CSA Z662 (Canadian Standards Association 2019), for pipe proper design in case the global buckling is harmful to the pipe.

The improvement of pipeline safety against seismic hazards remains a hot topic for the pipeline community and thus there is a significant ongoing research effort worldwide. The structural health assessment of pipelines under faulting is carried out using analytical tools (e.g. Karamitros et al. 2011; Sarvanis and Karamanos 2017; Talebi and Kiyono 2020), numerical modeling (e.g. Banushi et al. 2018; Demirci et al. 2018; Trifonov 2015; Vazouras et al. 2015), and experimental testing (e.g. Fadaee et al. 2020; Ha et al. 2010; Moradi et al. 2013; O'Rourke et al. 2016; Sarvanis et al. 2018; Tsatsis et al. 2019; Xie et al. 2013). Still, three analysis and design aspects require more attention by designers, operators, and researchers: (1) the calculation of the design fault displacement either via simplified deterministic approaches or full probabilistic fault displacement hazard analysis, (2) the critical details of the numerical modeling techniques that affect the reliability of the calculations, and (3) the alternative seismic countermeasures for the pipe protection. The critical state-of-the-art review of this study presents the available knowledge on these topics and mainly highlights the essential parameters that engineers and pipe operators should bear in mind to improve pipe safety and reliability. At the same time, the review shows the fields that are open to further research.

Design Fault Displacement

Structural codes provide a straightforward procedure for the estimation of the seismic loads for buildings and other above-ground structures, for example, EN 1998-1 (European Committee for Standardization 2004) and ASCE/SEI 7-10 (American Society of Civil Engineers 2010). On the other hand, pipeline codes lack specific provisions for the calculation of the design fault displacement, which is typically calculated via empirical fault scaling relations, featuring a deterministic approach. Davis (2008) has adopted the Wells and Coppersmith (1994) relations to estimate the design fault displacement (Δ) for water pipelines crossing tectonic faults. The displacement is estimated via the characteristic or the maximum earthquake magnitude (M) that is obtained from disaggregation results of a Probabilistic Seismic Hazard Analysis. Then, the displacement value is adjusted via correction factors (c) to account for the fault activity and the pipe function class. Briefly, the design fault displacement is estimated as (Thompson et al. 2018):

$$\Delta = c\Delta^*(M) \tag{1}$$

where Δ^* is either the maximum or the average fault displacement computed via the relation:

$$\Delta^* = a + bM \tag{2}$$

The use of empirical fault scaling relations is discussed indicatively by Dijkstra et al. (2021), O'Rourke and Liu (2012), and ASCE Guidelines (American Society of Civil Engineers 2011). Most engineers are familiar with the 30 years old relations of Wells and Coppersmith (1994), while recently Leonard (2014), and Thingbaijam et al. (2017) have published new relations using advanced statistical methods. These sets of expressions include relationships among fault characteristics and associated earthquakes, such as fault displacement, fault length, fault width, earthquake magnitude, etc. Most of these characteristics are specialized seismological information that engineers are not familiar with, apart from the fault length (L_F)

that can be obtained from a tectonic map or an available seismic hazard model. In such case, the fault displacement could be estimated via the (fault scaling) relation $\Delta \sim f(L_F)$ with respect to the fault mechanism, as presented in Table 2, where Δ is the average surface displacement and L_F is the fault length reported in geological or seismic hazard maps, being typically the subsurface. It should be noted that the Wells and Coppersmith (1994) estimation of the average displacement is based on the surface length (SL) that is typically lower than the subsurface length. In this case, the transformation $SL = 0.75L_F$ is used, as Wells and Coppersmith (1994) found that, on average, the surface rupture equals 75% of the subsurface rupture. Moreover, Leonard (2014) and Thingbaijam et al. (2017) provide a relation between the subsurface average fault displacement (Δ_{sub}) and the subsurface fault length. Based on the mode of the distribution ratios of average subsurface displacement to average surface displacement calculated by Wells and Coppersmith (1994), the transformation $\Delta_{sub} = 1.32\Delta$ is used to estimate the average surface fault displacement. A comparison of alternative empirical relations $\Delta \sim f(L_F)$ is presented in Fig. 2 within a fault length range of 10km$\leq L_F \leq$ 150km. As expected, a non-negligible variation is observed in the estimation of Δ values because each set of relations has been created using a different database, employing a different statistical method, and relying or not on a physical model (Wang 2018).

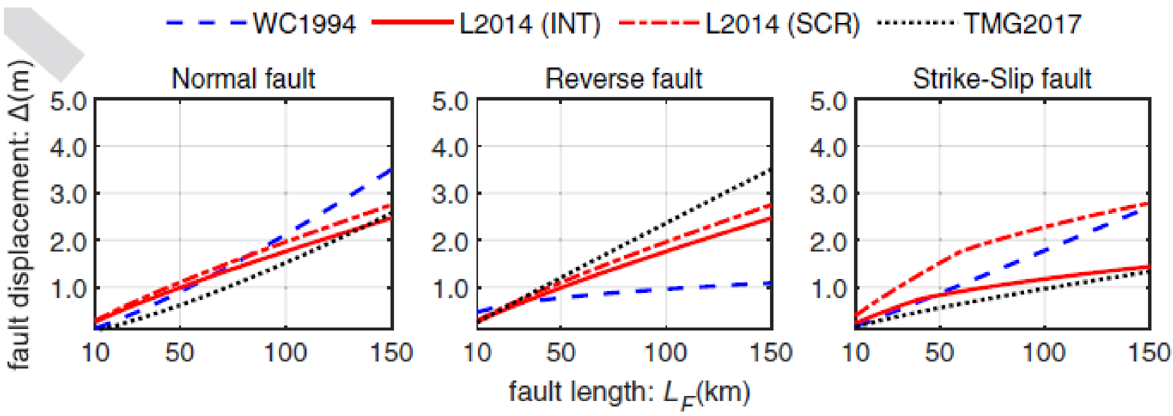

Fig. 2. Average fault displacement versus fault length via fault scaling relations. [Note: WC1994: Wells and Coppersmith (1994), L2014: Leonard (2014), TMG2017: Thingbaijam et

al. (2017), INT: interplate tectonic environment, and SCR: stable continental region tectonic environment.]

The estimation of the design fault displacement via fault scaling relations (deterministic approach) leads to an unknown level of conservatism and safety (Bommer 2002) because primarily the recurrence of the fault displacement is neglected. This recurrence might be taken into account indirectly via factors in a deterministic approach but still, it is a rough approach with many unquantified uncertainties. Additionally, there is no clear evidence, guidelines, or specific recommendations on using one over the other set of empirical relations for pipe design. In any case, these relations could provide a useful preliminary estimation of the displacement that the fault at hand might undergo based on its dimensions.

Pipeline networks are critical infrastructure and a performance-based framework (Cornell and Krawinkler 2000) is required to satisfy the resilience requirements (United Nations 2015). The full probabilistic treatment of the pipe–fault crossing problem in a rigorous scheme is a complex task and some attempts to work around the problem have been carried out. Strom et al. (2011) estimated the annual rate of rupturing displacement for pipeline design as the product of earthquake occurrence, surface rupturing during the earthquake, and pipeline being intercepted by the rupture probabilities. Cheng and Akkar (2017) have discussed the probabilistic fault displacement hazard via Monte Carlo Simulation. Recently, Ni et al. (2020) employed the Lasso regression, a machine learning technique, to develop fragility curves for pipes at fault crossings. A comprehensive framework for the performance-based assessment of pipelines at fault crossings has been presented by Melissianos et al. (2017b, 2021) using the Probabilistic Fault Displacement Hazard Analysis (PFDHA) of Youngs et al. (2003). The latter is an appropriate tool to quantify the probabilistic nature of earthquake faulting. The analysis provides the fault displacement hazard on the pipeline crossing site, namely the mean annual frequency of exceeding (λ_{Δ}) predefined fault displacement values (δ) via the expression:

$$\lambda_{\Delta}(\delta) = \nu_F \sum_i P(\Delta > \delta | m_i) P_M(m_i) \quad (3)$$

where ν_F is the recurrence rate of the fault, namely the annual average number of earthquake events with magnitude above a minimum one of engineering significance (M_{min}), $P(\Delta > \delta | m_i)$ is the probability that the fault displacement Δ exceeds a defined value δ at the crossing site, and finally $P_M(m_i)$ is the probability of magnitude *M* falling within the i-th bin, following an appropriate discretization of magnitude values between M_{min} and M_{max}. Parameters considered in the estimation of the probability $P(\Delta > \delta | m_i)$ are the fault mechanism, the fault length, the location of the crossing point on the fault trace, the maximum earthquake magnitude, and the probability of the rupture reaching the surface. This approach allows, also, the incorporation of aleatory and epistemic uncertainties. The former stem from the inherent variability of nature over time (e.g. earthquake magnitude, fault location) and may be handled via sampling. The latter originates from the inadequate understanding of nature (e.g. fault displacement prediction equations) and can be reduced in time with better observations while being typically handled for the time being via logic trees (Abrahamson and Bommer 2005).

The pipe design within a performance-based framework requires the definition of the appropriate intensity measure (IM), a quantity that indicates the level/magnitude of the earthquake and acts as an interface between seismology and structural engineering (Bakalis and Vamvatsikos 2018). In the case of ground shaking, an IM selection procedure is required for buried pipelines subjected to earthquake excitation (Tsinidis et al. 2020). Contrarily, it is pretty straightforward that the fault displacement is the appropriate scalar IM in the case of fault crossing, provided that duration-dependent failure modes, such as low-cycle fatigue, are not examined. Strictly speaking, the fault offset is generally three-dimensional (Fig. 3). Typically, the principal fault displacement component is much higher than the other two and determines the faulting mechanism. If the fault parallel component is the principal one, the faulting mechanism is strike-slip. In cases the fault perpendicular component is the principal one, the fault mechanism is normal or reverse (dip slip). Due to the lack of published data on the relationship between the fault displacement components, only reasonable engineering assumptions can be made (e.g. Melissianos et al. 2017b), leading to the introduction of a vector IM (Baker 2007). A brief overview of the performance assessment of a buried pipeline subjected to fault rupture is schematically shown in Fig. 4. The methodology comprises of three steps: (1) fault displacement hazard analysis, (2) pipeline structural analysis, and (3) pipeline strain hazard analysis. The outcome is the strain hazard curve that allows the evaluation of pipe performance in strain terms with respect to code-based strain limits and the design return period. The strain hazard curve is obtained via the convolution of results from steps (1) and (2). The uncertainties associated with demand (strains obtained from structural analysis) and capacity (code-based strain limits) have not been considered here for the sake of simplicity.

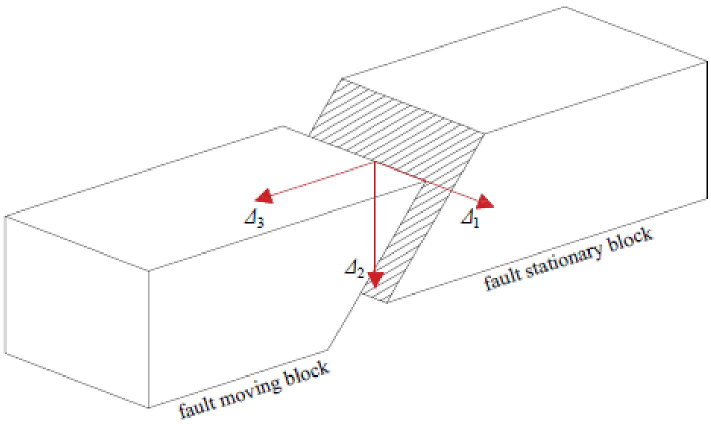

Fig. 3. Three-dimensional fault displacement, fault displacement components: Δ_1 fault-parallel, Δ_2 vertical, and Δ_3 perpendicular to the fault plane.

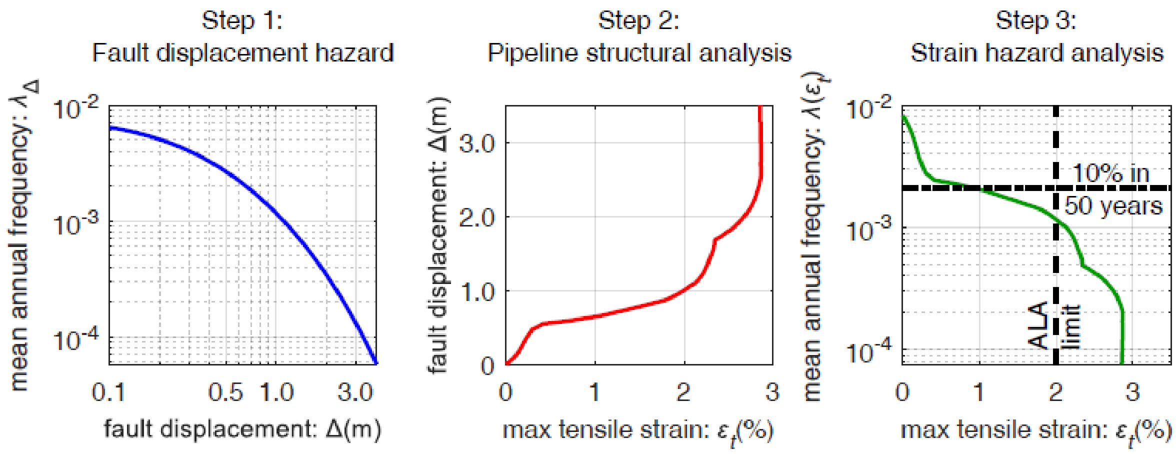

Fig. 4. Performance-based assessment of buried pipeline at fault crossing: A schematic illustration [adapted from Melissianos et al. (2017c)]

Alternative estimations of the design fault displacement using empirical relations and full probabilistic analysis are discussed via an illustrative example of three pipeline–fault crossings in Europe. The fault properties have been obtained from the fault database created for the development of the 2020 European Seismic Hazard Model (Danciu et al. 2019) within the EU-funded research project SERA (Giardini et al. 2017). A buried pipeline is considered to be intercepted by a fault with a length L_F and recurrence rate v_F, which is the average annual number of earthquake events above magnitude $M_{min} = 5.5$ of engineering significance. The pipeline is assumed to cross the fault at the middle of its length. The examined cases are: (A) a highly active normal fault close to Athens, capital of Greece with $L_F = 38.14\text{km}$ and recurrence rate $v_F = 0.0425\text{year}^{-1}$, (B) a very short strike-slip fault in the northern part of Turkey with length $L_F = 22.88\text{km}$ and $v_F = 0.0042\text{year}^{-1}$, and (C): a very long strike-slip fault in northwest France with $L_F = 159.74\text{km}$ and low seismicity (recurrence rate) $v_F = 0.0008\text{year}^{-1}$. For each one of the three cases, the (median average surface) fault displacement Δ is calculated based on the fault length via the relations of Table 2. Then, the displacement values that correspond to return periods (T) equal to 475years, 2000years, and 5000years are calculated from the hazard curves that are computed using the methodology of Melissianos et al. (2017b, 2021). The obtained fault displacements from the hazard curves (upper row of Fig. 5) are compared to the ones calculated using alternative fault scaling relations (lower row of Fig. 5). It is observed that the fault scaling relations should be used as an indication of the "expected" Δ based on the fault dimensions. Essentially, ignoring the fault productivity (recurrence rate) leads to an unknown safety level and conservatism. The fault in Case (A) has a high recurrence rate and thus the fault displacement values corresponding to return periods of 2,500 and 5,000 years are above 2 m, while the displacement values obtained from the scaling relations are roughly below 1 m because the fault length is small. Contrarily, the fault in Case (C) has a very low recurrence rate and the computed values are consequently low, while the displacements obtained from the scaling relations are excessive due to the length ($L_F =$ 159.74km). The fault in Case (B) is very short with a relatively low recurrence rate, leading to comparable values of fault displacement between the two approaches. All-in-all, one should be very careful when employing the empirical fault scaling relations, acknowledging the limitations and the potential inconsistency with the code-required design return period.

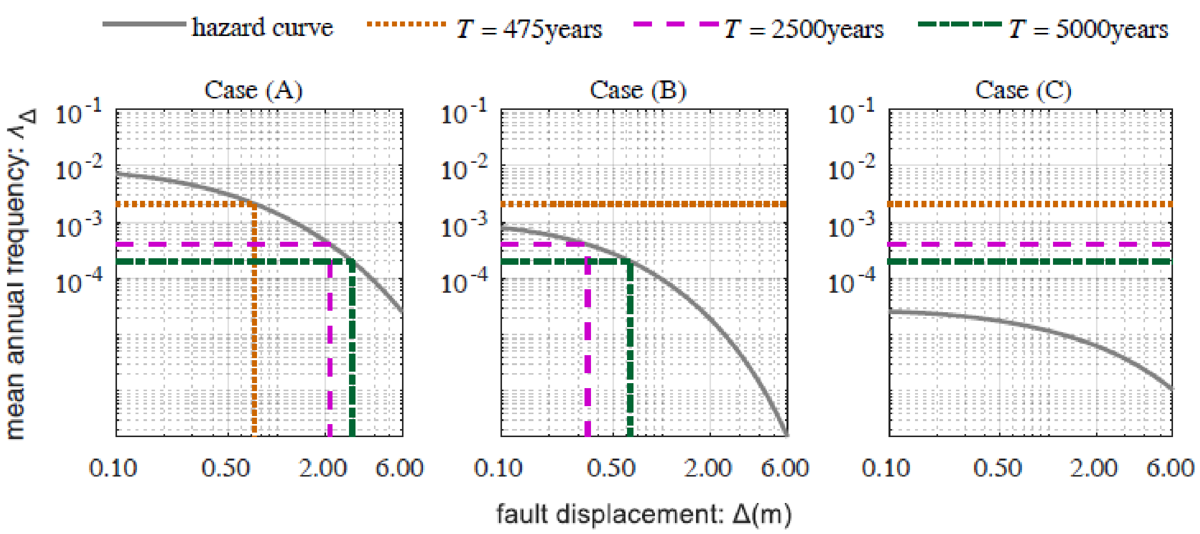

(a)

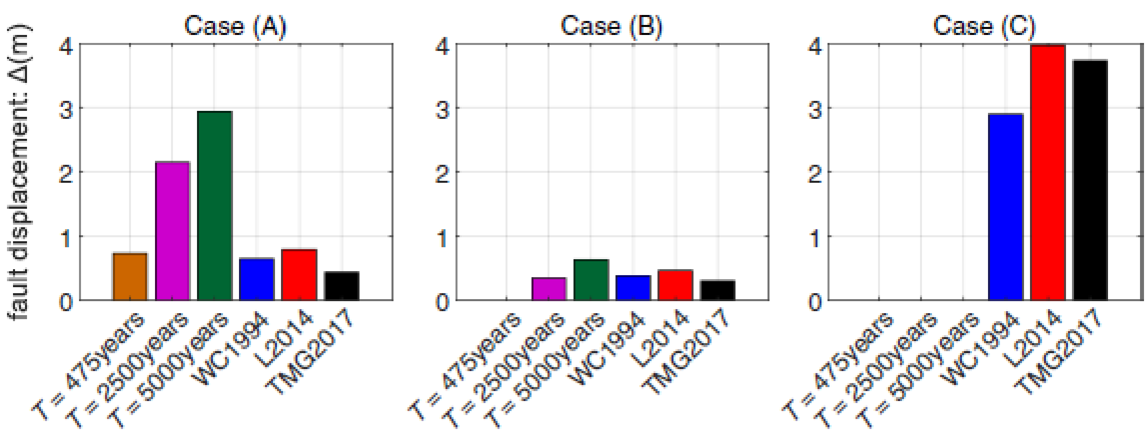

(b)

Fig. 5. Estimation of design fault displacement via empirical relations and probabilistic analysis [WC1994: Wells and Coppersmith (1994), L2014: Leonard (2014), TMG2017: Thingbaijam et al. (2017)].

Numerical modeling

The pipeline mechanical behavior due to faulting can be numerically evaluated by developing a beam-type or a continuum model (Xu et al. 2021). In more detail:

- Beam-type model: The pipeline is meshed into beam-type elements, allowing the calculation of stresses and strains at selected integration points on the cross-section and along the elements. The surrounding soil is modeled with non-linear translational springs in four directions: axial, transverse horizontal (lateral), vertical upwards, and vertical downwards. This model is presented in ASCE Guidelines, ALA Guidelines, EN 1998-4, CSA Z662 (Table 1) and adopted by researchers for the assessment of pipeline behavior (eg. Joshi et al. 2011; Melissianos and Gantes 2017; Trifonov 2018; Uckan et al. 2015). The beam-type model is routinely applied for the design of pipeline projects via commercial software, such as CAESAR II, AutoPIPE, and Rohr because the development is easy and fast.

- Continuum model: The pipeline is discretized into shell finite elements and the surrounding soil into 3D-solid elements. The pipe–soil interaction is modeled with contact elements. Starting from the innovative work of Vazouras et al. (2010), the continuum model is employed by researchers to gain in-depth knowledge of the pipe behavior (e.g. Gawande et al. 2019; Rahman and Taniyama 2015; Trifonov 2015; Vazouras et al. 2015) and to calibrate numerical models based on experimental results (Fadaee et al. 2020; Ni et al. 2018; Robert et al. 2016; Rofooei et al. 2018; Sarvanis et al. 2018; Tsatsis et al. 2019; Wijewickreme et al. 2017). It should be noted that continuum models are typically employed to estimate the pipe-soil interaction in a more accurate manner than the simplified beam-type models because the pipe-soil interface is modeled with contact elements that allow separation and sliding of the soil around the pipe. This approach, even though still subjected to several approximations, is the best available numerical approach to capture the physics of the problem, provided that the model is carefully developed and an appropriate soil material has been considered. Also, full-scale testing of buried pipelines subjected to faulting is undoubtedly difficult, costly, and time-consuming. Thus, limited experimental results are available and consequently, the validation of continuum numerical models is admittedly restrictive. Still, comparison to the few available experimental results increases the reliability of numerical results. Furthermore, non-linear springs might be used as an alternative for soil modeling instead of 3D-solid elements (e.g. Gantes and Bouckovalas 2013; Karamitros et al. 2007; Kouretzis et al. 2011; Talebi and Kiyono 2020; Xu and Lin 2017; Zhang et al. 2017). In such a case, special attention is required regarding the mesh density because, in the unlikely case of a coarse mesh, unrealistic local forces from springs acting on the shell might alter the local buckling estimations. The continuum model can be developed using general-purpose FEM software, such as Abaqus, ADINA, LS-DYNA, and ANSYS.

The selection of the appropriate modeling technique depends primarily on the required accuracy of the numerical predictions in terms of pipe local buckling and cross-section ovalization and secondary on the available computational resources and the experience of the pipeline engineer in advanced numerical modeling. One should bear in mind that a beam-type model can offer a reasonable estimation of the pipe–soil interaction until the local buckling occurrence (Karamanos et al. 2021). After that limit state, more advanced numerical models are required in terms of modeling the pipe with shell elements. The main advantages and disadvantages of each numerical approach are listed in Table 3.

Beam-type model

The critical aspect of pipe modeling as a beam resting on foundation (Winkler approach) is the force-displacement relationship of each soil spring, i.e. the numerical representation of the pipe–soil interaction. The industry-standard ALA Guidelines are typically used to estimate the soil spring properties. The basic inherent assumptions are that (1) the pipe is buried in uniform, dry, or fully saturated backfill, (2) the soil mechanical properties are independent of the stress level, and (3) the soil failure can freely develop, while the burial depth until the results are reliable is unknown (Kouretzis and Wu 2021).

Axial soil springs model the pipeline–soil friction with properties depending on backfill soil material and pipe coating. The maximum axial soil force per unit length can be estimated after ALA Guidelines based on geotechnical approaches that are used to model the force transfer on axially loaded piles (Singhal 1980):

$$T_u = \pi D a c + \pi D H \bar{\gamma} \frac{1 + K_0}{2} \tan\delta \tag{4}$$

where D is the pipe diameter, a is the adhesion factor, c is the soil cohesion representative of the soil backfill, H is the depth to the pipe centerline, $\bar{\gamma}$ is the effective unit weight of the soil, K_o is the coefficient of pressure at rest, and δ is the interface angle of friction for pipe and soil that depends on the internal friction angle of the soil and the type of pipe coating. The maximum displacement depends on the soil type. Wijewickreme et al. (2009) performed full-scale axial pull-out tests of pipes buried in dry sand. The axial load was found to be similar to the one predicted by ASCE Guidelines for loose sand, while it was found much higher for dense sand. In cases of dilatant sandy soil (e.g. in compacted trenches), the authors noted that the use of existing code relations may lead to the underestimation of soil loads. Meidani et al. (2017) performed axial pull-out tests and discrete element analyses on pipes embedded in dense sand. It was shown that the axial resistance was higher than the one predicted by ASCE Guidelines because the dense sandy soil surrounding the pipe was not at rest, implying that the actual pressure coefficient should be higher than K_o for relatively dense sand material. Sarvanis et al. (2018) performed axial pull-out full-scale tests and proposed an updated version of the ASCE Guidelines to take consider the stress increase at the pipe interface. This increase is related to the fact that the sand backfill might not freely expand due to confined shear conditions caused by sand dilatancy. Recently, Marino and Osouli (2020) performed an experimental campaign on the slip resistance of coal tar-coated buried pipes in clay and sand. The authors concluded that more analysis and testing is required on the coating (reduction) factors due to their dependency on soil type and the unsaturated soil strength should be considered if that is the soil case. To sum up, it should be considered for the design that if the backfill is purposely compacted (e.g. under road crossings), considering the "at-rest" lateral earth pressure coefficient K_0 would result in decreased axial loads on the displaced pipe (potentially unsafe condition) and consequently to lower strains within the zone of ground deformation. In brief, in the case of dense sand backfill, the axial soil resistance would be higher than the one predicted by codes. However, more experimental and numerical analyses are required to formulate an updated expression for axial soil resistance for code implementation.

Transverse horizontal (lateral) springs model the soil resistance to pipe lateral movement in the trench. This mechanism has been considered to be similar to one of vertical anchor plates or horizontal moving foundations by passive earth pressure (Trautmann and O'Rourke 1983). This approach assumes that the soil failure could be fully developed or in other words the trench geometry and the native soil (outside the trench) do not affect the development of soil failure surfaces. A qualitative statement is only included in ALA Guidelines, stating that the trench dimensions shall be "adequate", i.e. the trench and the surrounding native soil can be regarded as "infinite" free-field conditions. The maximum lateral soil force may be estimated after ALA Guidelines as:

$$P_u = N_{ch} c D + N_{qh} \bar{\gamma} H D \tag{5}$$

where N_{ch} is the horizontal bearing capacity factor for clay, N_{qh} is the horizontal bearing capacity factor. The displacement corresponding at P_u is a linear function of burial depth and pipe diameter. Regarding the effect of trench geometry in the development of the soil failure surfaces, Kouretzis et al. (2013) carried out a numerical study to investigate the shape and size of the failure surface for pipes being laterally displaced in loose and medium-density sand backfills. Chaloulos et al. (2015) employed 2D finite element modeling and examined laterally displaced pipelines. The authors identified three failure mechanisms for loose to medium density sand backfills concerning the bural depth to diameter ratio, namely shear failure, local shear failure, and intermediate shear failure modes. Chaloulos et al. (2017) extended their previous work and developed a straightforward analytical methodology for the computation of the soil pressure applied on a laterally displaced pipeline concerning the trench geometry and shape (width and wall inclination). A set of modification factors was developed for design in case the trench is excavated in stiff soils and rocks. Then, pipeline–soil lateral interaction remains a topic under investigation via experimental tests and detailed numerical models.

Notable experimental and numerical studies have been conducted during the last decade, which highlight the need for code revision. Tian and Cassidy (2011) developed a pipe–soil interaction model for a pipe under horizontal and vertical loading and introduced a radial hardening term that was found to be necessary for pipes being horizontally displaced twice their diameter due to accumulated soil berm. Daiyan et al. (2011) conducted centrifuge tests and FE analysis, concluding that the lateral soil force depends on the movement angle of the pipe in the trench to soil friction angle and burial depth. Jung et al. (2013) performed a combination of physical tests and FE analysis showing that the dimensionless maximum lateral force mobilized by large-diameter pipes buried in dense sand is decreased at low depth to diameter ratios. Roy et al. (2016) employed FE modeling to analyze the pipe–soil interaction using a Modified Mohr-Coulomb soil model, aiming to replicate experimental results and to investigate the effects of pipe diameter, burial depth, and soil properties. Robert et al. (2016) carried out experimental tests and numerical analyses and found that if a pipeline is buried in unsaturated sand, then soil lateral resistance is higher than anticipated and should be considered in the analyses. Ono et al. (2017) conducted lateral loading experiments in pipes buried in sand focusing on the influence of the initial effective stress. The authors developed a force–displacement relationship to account for the variation of soil unit weight concerning pore water pressure, burial depth, pipe diameter and length. Robert (2017) developed a modified Mohr-Coulomb model to simulate the behavior of pipes in unsaturated soils because soil friction affects the lateral loads imposed on pipes. Roy et al. (2018a) performed numerical analyses of laterally loaded pipes in dense sand and revealed that the peak and residual resistances increase with the embedment ratio until a critical value that depends on the pipe diameter. Nguyen and Asimaki (2018) proposed a modified uniaxial Bouc-Wen model to evaluate the force–displacement backbone curve for the lateral interaction of pipe–sandy soil. Chakraborty (2018) numerically examined pipes embedded in a cohesive soil and showed that the lateral soil capacity decreases with the decrease of pipe burial depth to diameter ratio and soil friction angle. Tahamouli Roudsari et al. (2019) experimentally investigated pipes under strike-slip faulting using a shear box and found that the maximum lateral soil force was 70% higher than the one estimated after ASCE Guidelines and close to the one estimated after ALA Guidelines for steel pipes. In the case of HDPE pipe, the force was 80% lower than ASCE Guidelines, demonstrating that the code expression should be adjusted to incorporate the effect of pipe material. Recently, Wu et al. (2020) carried out tests to investigate the transition from a shallow to a deep failure mechanism concerning pipe burial depth and friction angle. Ashrafy et al. (2020) proposed a modification of ASCE Guidelines and ALA Guidelines equations for lateral soil resistance for thick pipes buried in dense sand and subjected to strike-slip faulting. Dilrukshi and Wijewickreme (2020) examined the influence of the particle size of soil backfill material with respect to the pipe size and formed a relation for the peak lateral force considering burial depth to diameter and pipe diameter to soil particle size ratios. The authors formulated an expression for practical application in pipe design. Finally, Ansari et al. (2021) performed small-scale tests in a soil chamber to investigate the soil resistance to pipe lateral movement in loose to very dense dry sand. The authors concluded that the existing equations for dense sand backfill underestimate the lateral soil resistance. Summarizing, the following main remarks should be considered regarding the lateral soil force–displacement relationship:

- Code relations assume “free-field” conditions or in other words, it is assumed that the failure surface is developed within the trench. If these assumptions are not satisfied, then appropriate modification factors should be applied to the code relations. The analytical approach of Chaloulos et al. (2017) to compute the trench size and shape effect could be practically employed for pipeline design. The methodology is outlined in Table 4.
- The lateral soil resistance of unsaturated sand is higher than expected. Code relations should be modified for pipe material other than steel. There are preliminary findings that the

movement angle of the pipe in the trench affects the soil force. Finally, soil resistance to pipe lateral movement is underestimated in dense sandy backfill.

Vertical upward springs model the uplift soil resistance due to the upward movement of the pipe in the trench. The maximum soil force corresponds to the weight of an inverted prism of soil above the pipeline top (O'Rourke and Liu 2012). The maximum vertical uplift soil force may be estimated after ALA Guidelines:

$$Q_u = N_{cv} c D + N_{qv} \bar{\gamma} H D \tag{6}$$

where N_{cv} is the vertical uplift factor for clay, N_{qv} is the vertical uplift factor for sand. The corresponding displacement at Q_u is a linear function of burial depth and depends on the pipe diameter and soil type. There is significant research effort on the uplift soil mechanisms of buried offshore pipelines in light of preventing thermal upheaval buckling. Contrarily, the number of studies for onshore pipelines during the last decade is limited. Jung et al. (2013a) performed 2D FE analyses to examine the uplift pipe–sandy soil interaction and developed hyperbolic and bilinear relations for the uplift force–displacement curves taking into account the density and the burial depth to diameter ratio. Chakraborty and Kumar (2014) performed FE analyses and examined the variation of friction angle in the soil domain concerning the sandy soil type, the burial depth, and the pipe diameter. Robert and Thusyanthan (2018) examined the uplift resistance of buried pipes in partially saturated sand because the latter is not considered in the existing expressions. The authors performed tests in a soil chamber and found that the uplift resistance of deeply buried pipes in denser soils is lower than the one obtained from ASCE Guidelines. A model was proposed to evaluate the uplift resistance of small diameter pipes in partially saturated sand. Wijewickreme et al. (2017) executed full-scale experiments modeling pipes under reverse faulting to evaluate the soil mobilization due to the pipe upward movement in the trench with respect to fault dip angle and soil friction angle. The authors proposed modifications to existing expressions (soil springs) regarding the distance from the fault trace. Roy et al. (2018) proposed a modified Mohr-Coulomb law for design applications regarding the uplift resistance by considering the effect of burial depth on the developed failure surfaces, the inversely proportional relation between displacement and burial depth, and the decrease of uplift resistance at large displacements with the increase of upward movement. Wu et al. (2020b) performed a series of physical tests and concluded that the existing relations should be used with caution even for shallowly buried pipes because the failure mechanism is almost independent of sand density. Very recently, Cugnetto et al. (2021) employed FE modeling of pipes buried in dry sand, using advanced soil material laws. The authors found the simplified linear elastic-perfectly plastic Mohr-Coulomb material law can be used to safely estimate the upward soil resistance. The code expressions yield conservative results (overprediction) for deeply buried pipelines, while for shallowly buried ones, the corresponding results are acceptable. To summarize, current expressions yield conservative results due to the interaction between the pipe burial depth, the pipe upward movement, and the uplift mobilized soil force.

Pipe vertical downward movement results in the development of forces at the pipe–soil interface that corresponds to the vertical bearing capacity of a footing (O'Rourke and Liu 2012). The maximum vertical downward soil force after ALA Guidelines is:

$$Q_d = N_c c D + N_q \bar{\gamma} H D + N_\gamma \gamma D^2/2 \tag{7}$$

where N_c, N_q, N_γ are bearing capacity factors and γ is the total unit weight of soil. The maximum displacement is a linear function of the pipe diameter and depends on soil cohesion. Xie et al. (2013) numerically examined pipes subjected to normal faulting and found that the bearing capacity was 1/8 the value estimated after ASCE Guidelines and the bearing capacity variated along the pipe, with the lower value found close to the fault plane. An update of code expressions was provided. Kouretzis et al. (2014) proposed an updated set of expressions for computing the downward soil resistance because the existing ones in ALA Guidelines can significantly underestimate or overestimate the soil resistance. The authors gave practical suggestions regarding the trench dimensions to avoid the interaction between the soil failure surface and the potentially stiffer native soil. O'Rourke et al. (2016) examined the response of pipelines subjected to vertical ground movement, reviewed measured stress of pipe in full-scale tests, and discussed the pipeline–soil interaction under normal faulting taking into account the coupling of frictional forces and soil reaction forces normal to the pipeline axis. It was concluded that the maximum downforce is about 1/3 the one derived from existing equations. Jung et al. (2016) carried out full-scale tests of pipes under faulting and numerical analyses to examine soil restrains. The maximum downward force was found to be 1/3 of the corresponding one after existing equations, rendering code provisions as overly conservative. Also, the pipe diameter was a parameter affecting soil force for constant burial depth, i.e. increasing the diameter led to increasing soil stresses. Recently, Qin et al. (2019) numerically examined rigid pipes embedded in granular soil and subjected to downward movement. The authors found that the code expressions overestimate the bearing capacity and proposed a new force–displacement relation based on the local shear failure theory, compared to the general shear failure theory adopted by codes. Cugnetto et al. (2021) focused on the investigation of the downward soil resistance of buried pipelines embedded in dry sand and subjected to vertical fault movement. The continuum FE model was employed and it was noticed that simplified linear elastic-perfectly plastic Mohr-Coulomb material law can be used to safely estimate the downward soil resistance. Contrarily, it was verified that the code expressions are over-conservative. The authors built a statistical model (fitting expression) based on the numerical results for predicting the soil downward resistance force with respect to the pipeline length, the embedment ratio, and the soil properties for pipes buried in noncohesive, dense to loose, and dry homogenous sand material. Summarizing, it is concluded that the code relations for estimating the soil downward resistance provide overestimations, leading to conservative pipe design and highlighting the need for revision. Regarding the trench geometry, as stated by Kouretzis et al. (2014), the higher the burial depth and the soil friction angle, the larger the cross-section area of the trench should be in terms of both with and wall inclination. This is to allow the formation of the soil failure modes. Otherwise, a cost-benefit analysis is required to compare the cost of additional excavations and the implementation of mitigation measures.

Finally, the recent study of Kouretzis and Wu (2021) presents a comprehensive and complete set of recommendations for the estimation of the lateral and vertical soil spring properties based on a set of new experimental results by Ansari et al. (2018). The updated expressions take into account the dependency of sand properties on the confining stress levels. The response of typical buried steel pipelines in terms of strains was evaluated using the ALA Guidelines and the updated expressions for soil spring properties. It was found that in the former case, pipe strains were significantly higher, demonstrating the conservatism of ALA estimations. The proposed set of expressions is listed in

Table 5 for potential design application.

Continuum model

The pipe–fault crossing analysis with a continuum numerical model allows among others to assess the pipe local instability (shell buckling) and cross-section ovalization, model the trench cross-section shape, and use advanced soil material laws. However, the model length is limited and the pipe segments beyond the curved length and until the anchor points should be represented using a simplified approach. These three aspects are discussed in detail subsequently.

Trench geometry is typically not considered in the analysis assuming that the pipe is buried in homogeneous soil and consequently soil failure surfaces can freely develop. Still, if the trench is excavated in stiff or rocky soil, then modeling the trench geometry is required, as discussed by Trifonov (2015) and Cheng et al. (2019).

An elastic–perfectly plastic Mohr-Coulomb law is typically employed for soil modeling (e.g. Soveiti and Mosalmani 2020; Vazouras et al. 2015). Trifonov (2015) adopted a Drucker-Prager criterion to avoid the computational difficulties associated with corners at the yield surface of the Mohr-Coulomb law. Experimental results could, also, be used for the development of custom-made laws (e.g. Dey et al. 2020). Recently, Robert et al. (2020) developed codes for practical application in commercial software to model the pipeline–soil interaction, focusing on dry and unsaturated soils.

Modeling a very long segment of the pipeline is not viable because excessive computational resources are required. Thus, Vazouras et al. (2010) suggested a modeling length equal to 60 times the pipe diameter. The boundary conditions at the pipeline ends play a non-negligible role and affect the pipeline behavior, a task that can be handled via alternative approaches:

- The pipeline beyond the continuum model is replaced by an equivalent spring to consider the axial deformation of the pipe. Liu et al. (2004) discussed this topic and developed an equivalent spring via a simplified approach. Vazouras et al. (2015) developed an equivalent spring for an infinitely long pipeline and a finite-length pipeline by analyzing separately the sliding and the non-sliding segment (inelastic and elastic behavior at the pipe–soil interface, respectively) of the pipeline. Zhang et al. (2016b) update the model of Liu et al. (2004), introducing discrete cases along the straight segment of the unanchored length regarding pipe steel yielding (elastic and inelastic pipe behavior) and yielding of axial springs. Recently, Banushi and Squeglia (2018) provided an advanced methodology for estimating the force–displacement relation of the equivalent springs for pipelines subjected to strike-slip faulting, considering the pipeline operating temperature and the internal pressure and providing different relations for tension and compression. To summarize, the available methodologies for computing the properties of the equivalent spring require detailed calculations for each segment of the force–displacement relationship. The required pipe–soil interaction parameters can be obtained from either experimental tests or additional advanced numerical analyses of pipe pull-out loading. The soil stiffness and the shear strength at the pipe–soil interface are required in the methodology of Vazouras et al. (2015). The properties of the equivalent spring after the methodology of Banushi and Squeglia (2018) are a function of soil and pipeline nonlinear properties, elastic rigidity of pipe–soil friction interaction, internal pressure and temperature variation, pipeline unanchored length, and pipe cross-section area. Contrarily, the methodology of Zhang et al. (2016b) seems simpler, requiring the pipe cross-section area, the steel modulus of elasticity, and the maximum axial soil spring force along with the corresponding yielding displacement (both might be obtained from ALA Guidelines). It is noted that each methodology was founded on different assumptions and consequently a direct comparison is not viable.

- The pipeline segment beyond the continuum model is modeled with the beam-type model (e.g. Gantes and Bouckovalas 2013; Zeng et al. 2019), connecting the two parts (continuum and beam-type model) via rigid links.

Protection Measures

The protection of buried pipelines at fault crossing results from a blend of regulatory provisions (Table 1), engineering judgment (e.g. Darigo et al. 2008; Keaton and Honegger 2008), and requirements of the pipeline owner. The general regulatory recommendations are (1) pipe rerouting to avoid environmentally sensitive and populated areas, (2) pipe orientation (selection of pipe–fault crossing angle) that results in pipe tension, rather than compression, (3) minimization of burial depth to reduce soil restrains on the pipe during movement in the trench, (4) avoidance of sharp bends in the crossing area that might act as anchor points (Nair et al. 2019), and (5) trench backfilling with appropriate soil material over a distance of 50m on each side of the fault trace. These recommendations stand as the “first line of defense” against the consequences of faulting but might not be sufficient enough to ensure the pipe safety or not applicable due to environmental restrictions, the presence of physical obstacles, and regulatory restrictions. Thus, specific seismic countermeasures are typically required, the selection of which is based on a cost-benefit analysis using appropriate variables, such as procurement and installation cost, pipe–fault crossing geometry, pipe owner specifications, and regulatory provisions.

The protection of buried pipes at fault crossings might be seen as a trivial or very broad issue that is handled on a case-by-case basis. Nevertheless, a comprehensive and critical review of the international engineering practice remains useful for designers and pipe owners. At the same, it should be noted that the literature on pipeline protection measures is very limited compared to pipeline mechanical behavior studies. Qualitative discussions on protection measures are offered by Nyman et al. (2008), O’Rourke and Liu (2012), and Karamanos et al.

(2017). Quantitative comparisons of measures are presented by Gantes and Melissianos (2016), Melissianos et al. (2017c), Melissianos and Gantes (2019), and Valsamis et al. (2020). In these studies, the authors have grouped the measures into three categories, based on the mechanism employed to achieve pipe strain reduction: pipe strengthening, soil friction reduction, and complex measures.

Types of protection measures

Pipe strengthening can be achieved by:

- Steel grade upgrade to improve strength (Gantes and Bouckovalas 2013; Karamanos et al. 2017),
- Wall thickness increase to improve pipe cross-section stiffness (Gantes and Bouckovalas 2013; Karamanos et al. 2017).
- Pipe wrapping with composite wraps to increase strength (Mokhtari and Alavi Nia 2015; Trifonov and Cherniy 2014, 2016).

The reduction of the friction developed on the pipe-soil interface contributes to the reduction of pipe strains. This could be accomplished by the:

- Trench backfilling with tire-derived aggregate, which is a compressible material (Ni et al. 2018; Sim et al. 2012).
- Use of geotextile-lined pipeline trenches (Gantes and Bouckovalas 2013) that have a marginal effect on pipelines subjected to strike-slip faulting (Monroy-Concha et al. 2012).
- Trench backfilling with loose granular soil, for example, pumice (Gantes and Bouckovalas 2013; Valsamis et al. 2020).
- Excavation of a wider trench for the pipeline to "freely" move in the trench (Gantes and Bouckovalas 2013).

- Pipe isolation from ground displacements by placing the pipeline within concrete culverts and without backfilling material in the case of strike-slip faulting (Gantes and Bouckovalas 2013; Tsai et al. 2015; Valsamis et al. 2020).
- Partial replacement of soil backfill with EPS geofoam blocks (Azizian et al. 2020; Bartlett et al. 2015; Beju and Mandal 2017; Choo et al. 2007; D.G. Honegger Consulting SSD Inc. 2009; Rasouli and Fatahi 2020).

Other measures that have been proposed by scholars or applied on a case-specific basis and can be classified neither as pipe strengthening nor as friction reduction are listed below:

- Zhang et al. (2016) examined a protective device that aims at reducing the potential of local buckling by applying external hydrostatic pressure to the pipeline at critical predefined locations.
- Besstrashnov and Strom (2011) proposed a pipe route changing with a very high radius bend to allow unrestrained pipe deformation.
- Melissianos et al. (2016, 2017a), Valsamis et al. (2020), and Valsamis and Bouckovalas (2020) have investigated the use of flexible joints as a novel design approach. Flexible joints are introduced in the pipeline at the fault vicinity to “absorb” pipe deformation and render pipe segments virtually undeformed and consequently unstrained. The structural system of the pipeline is transformed from continuous to segmented because the joints “act” as internal hinged. The commercial bellow-type joints are welded between pipe segments, thus ensuring pipe continuity and excluding the risk of separation, which is a typical failure mode of low-pressure segmented pipes. Experimental, analytical, and numerical studies carried out by the authors have revealed that it is a very promising solution especially for pipes being subjected to significant fault offset displacement.
- Hart et al. (2004) designed a case-specific pipeline–fault crossing consisting of a pipe offset made of four cold high-radius bends.

- Vazouras and Karamanos (2017) investigated the potential use of field bends as a mitigation measure to relieve pipe strains under very specific conditions, taking advantage of bends' flexibility.
- Hasegawa et al. (2014) proposed the creation of a predefined buckling pattern that consists of localized deformation of the pipe wall at specified predefined locations aiming at controlling the pipe local deformation (Wham et al. 2019).

Finally, if no measure is efficient enough, the pipe might be elevated above the ground, a solution that has been applied successfully at the Trans-Alaska – Denali Fault crossing (Honegger et al. 2004).

The comparison of "conventional" measures presented by Gantes and Melissianos 2016; Melissianos et al. 2017c; Melissianos and Gantes 2019; Valsamis et al. 2020 yields the following results for practical consideration:

- Pipe strengthening measures (wall thickness increase and steel grade upgrade) are economically acceptable only for low to very low fault displacement ($\Delta < 1.0D$).
- Trench backfilling with fine-graded soil material is, in general, an efficient measure for medium to high fault displacement ($1.0D < \Delta < 3.0D$).
- Pipe placement within culverts is a very expensive but efficient measure for very high strike-slip fault displacement ($\Delta > 3.0D$).
- Pipe–fault crossing angle and fault dip angle are predominant parameters affecting the effectiveness of protection measures.

Selection criteria

The selection of the appropriate protection measure is based on a set of criteria given the current legislation and the pipe owner's specifications. The categorical criteria set by Valsamis et al. (2020) are adopted to group the parameters that drive the selection and formulate a set of preliminary selection criteria (Table 6), which should be considered under the following remarks:

- Protection measures are applied along the entire fault trace uncertainty length, thus affecting the cost-related criteria.
- Weight factors should be applied if necessary, depending on the case at hand. For example, if the crossing is located at a remote mountainous site, the transportation and installation costs might be very high.
- More than one protection measure might be selected to satisfy the design objectives.

Five protection measures, namely wall thickness increase (pipe strengthening), pipe placement within culverts and backfilling with pumice (soil friction reduction), and introduction of flexible joints and route changing with high radius bends (complex) are indicatively examined using the selection criteria of Table 6. The compliance of each measure to every criterion is presented in Table 7, demonstrating that the selection process is a multi-level cost-benefit analysis. Regarding the criterion "1.4 Requirement for sophisticated analysis" of Table 6, brief practical guidelines for the numerical modeling of alternative protection measures are offered in Table 8.

Conclusions

The performance of onshore buried steel fuel pipelines at fault crossings has been studied extensively during the past years. Still, some aspects require the attention of the scientific community. The state-of-the-art review presented has critically examined three topics: the estimation of the design fault displacement, the critical numerical modeling aspects to be considered in the design, and the selection of pipe protection measures. The main findings are summarized as follows:

- Empirical fault scaling relations should be used as an indication or a deterministic cap of the design fault displacement. A full probabilistic Figure analysis is suitable for estimating the design fault displacement and achieving a balance between safety and economy.
- In case a beam-type numerical model is developed for the analysis of the pipe–fault crossing, attention should be paid to the force–displacement curves for the soil springs provided in codes. The engineer should be aware of the code assumptions and restrictions because there are cases in terms of soil properties, loading conditions, etc. that these curves lead to either conservative and expensive or unsafe pipe design. There are recently published expressions for the lateral, vertical upward, and vertical downward soil springs' force–displacement curves that could be used in the design.
- In case a continuum numerical model is developed for the pipe analysis, an available methodology should be considered to replace the pipe segments between the curved length and the anchor points.
- The relationship between backfill and the native soil properties, as well as the trench geometry in the case of significant lateral movement of the pipe, should drive the decision on considering or not the trench cross-section shape in the numerical model.
- A variety of conventional and case-specific protection measures is available, which aim at pipe strain reduction via pipe strengthening, soil friction reduction, or more complex mechanisms. The selection of a protection measure results from a cost-benefit analysis. A set of preliminary selection criteria has been developed for practical application, where partial weight factors should be applied based on engineering judgment and a case-by-case basis.

Data availability statement

Some or all data, models, or code that support the findings of this study are available from the corresponding author upon reasonable request.

Acknowledgments

The partial financial support provided by the European Union's Horizon 2020 research and innovation programmes "INFRASTRESS – Improving resilience of sensitive industrial plants & infrastructures exposed to cyber-physical threats, by means of an open testbed stress-testing system" under grant agreement No. 833088 and "HYPERION – Development of a Decision Support System for Improved Resilience & Sustainable Reconstruction of historic areas to cope with Climate Change & Extreme Events based on Novel Sensors and Modelling tools" under Grant Agreement No. 821054 is gratefully acknowledged.

References

Abdulhameed, D., Cakiroglu, C., Lin, M., Cheng, R., Nychka, J., Sen, M., and Adeeb, S. (2016). "The Effect of internal pressure on the tensile strain capacity of X52 pipelines with circumferential flaws." *Journal of Pressure Vessel Technology*, 138(6), 1–18.

Abrahamson, N. A., and Bommer, J. J. (2005). "Probability and uncertainty in seismic hazard analysis." *Earthquake Spectra*, 21(2), 603–607.

American Lifelines Alliance. (2001). *Guidelines for the design of buried steel pipe*. National Institute of Building Sciences, Washington, DC, USA.

American Society of Civil Engineers. (1984). *Guidelines for the seismic design of oil and gas pipeline systems*. New York, NY, USA.

American Society of Civil Engineers. (2010). *ASCE/SEI 7-10 Minimum design loads for buildings and other structures*. Reston, VA, USA.

American Society of Civil Engineers. (2011). *Guidelines for seismic evaluation and design of petrochemical facilities*. Reston, VA, USA.

American Society of Mechanical Engineers. (2018). *ASME B31.8-2018 Guide for gas transmission and distribution piping systems*. New York, NY, USA.

Ansari, Y., Kouretzis, G., and Sloan, S. W. (2018). “Development of a prototype for modelling soil–pipe interaction and its application for predicting uplift resistance to buried pipe movements in sand.” *Canadian Geotechnical Journal*, 55(10), 1451–1474.

Ansari, Y., Kouretzis, G., and Sloan, S. W. (2021). “Physical modelling of lateral sand–pipe interaction.” *Géotechnique*, 71(1), 60–75.

Ashrafy, M., TahamouliRoudsari, M., and Hosseini, M. (2020). “New formulation for establishing the lateral interaction between buried steel pipeline and sandy soil subjected to strike-slip faulting.” *Journal of Pressure Vessel Technology, Transactions of the ASME*, 142(2), 1–17.

Azizian, M., Tafreshi, S. N. M., and Darabi, N. J. (2020). “Experimental evaluation of an expanded polystyrene (EPS) block-geogrid system to protect buried pipes.” *Soil Dynamics and Earthquake Engineering*, 129, 105965.

Bakalis, K., and Vamvatsikos, D. (2018). “Seismic fragility functions via nonlinear response history analysis.” *Journal of Structural Engineering*, 144(10), 1–15.

Baker, J. W. (2007). “Probabilistic structural response assessment using vector-valued intensity measures.” *Earthquake Engineering & Structural Dynamics*, 36(13), 1861–1883.

Banushi, G., and Squeglia, N. (2018). “Seismic analysis of a buried operating steel pipeline with emphasis on the equivalent-boundary conditions.” *Journal of Pipeline Systems Engineering and Practice*, 9(3), 04018005.

Banushi, G., Squeglia, N., and Thiele, K. (2018). “Innovative analysis of a buried operating pipeline subjected to strike-slip fault movement.” *Soil Dynamics and Earthquake Engineering*, 107, 234–249.

Bartlett, S. F., Lingwall, B. N., and Vaslestad, J. (2015). “Methods of protecting buried pipelines and culverts in transportation infrastructure using EPS geofoam.” *Geotextiles and Geomembranes*, 43(5), 450–461.

Beju, Y. Z., and Mandal, J. N. (2017). "Combined use of jute geotextile-EPS geofoam to protect flexible buried pipes: Experimental and numerical studies." *International Journal of Geosynthetics and Ground Engineering*, 3, 32.

Besstrashnov, V. M., and Strom, A. L. (2011). "Active faults crossing trunk pipeline routes: Some important steps to avoid disaster." *Natural Hazards and Earth System Science*, 11(5), 1433–1436.

Bommer, J. J. (2002). "Deterministic vs. probabilistic seismic hazard assessment: An exaggerated and obstructive dichotomy." *Journal of Earthquake Engineering*, 6, 43–73.

Canadian Standards Association. (2019). *Z662:19 Oil and gas pipeline systems*. CSA, Etobicoke, Canada.

Chakraborty, D. (2018). "Lateral resistance of buried pipeline in c-φ soil." *Journal of Pipeline Systems Engineering and Practice*, 9(1).

Chakraborty, D., and Kumar, J. (2014). "Vertical uplift resistance of pipes buried in sand." *Journal of Pipeline Systems Engineering and Practice*, 5(1), 04013009.

Chaloulos, Y. K., Bouckovalas, G. D., and Karamitros, D. K. (2017). "Trench effects on lateral p-y relations for pipelines embedded in stiff soils and rocks." *Computers and Geotechnics*, 83, 52–63.

Chaloulos, Y. K., Bouckovalas, G. D., Zervos, S. D., and Zampas, A. L. (2015). "Lateral soil-pipeline interaction in sand backfill: Effect of trench dimensions." *Computers and Geotechnics*, 69, 442–451.

Cheng, X., Ma, C., Huang, R., Huang, S., and Yang, W. (2019). "Failure mode analysis of X80 buried steel pipeline under oblique-reverse fault." *Soil Dynamics and Earthquake Engineering*, 125, 105723.

Cheng, Y., and Akkar, S. (2017). "Probabilistic permanent fault displacement hazard via Monte Carlo simulation and its consideration for the probabilistic risk assessment of buried continuous steel pipelines." *Earthquake Engineering & Structural Dynamics*, 46, 605–620.

Choo, Y. W., Abdoun, T. H., O'Rourke, M. J., and Ha, D. (2007). "Remediation for buried pipeline systems under permanent ground deformation." *Soil Dynamics and Earthquake Engineering*, 27(12), 1043–1055.

Cornell, C. A., and Krawinkler, H. (2000). "Progress and challenges in seismic performance assessment." *PEER Center News*, 3(2), 1–4.

Corona, E., and Kyriakides, S. (1991). "An experimental investigation of the degradation and buckling of circular tubes under cyclic bending and external pressure." *Thin-Walled Structures*, 12(3), 229–263.

Corona, E., and Kyriakides, S. (2000). "Asymmetric collapse modes of pipes under combined bending and external pressure." *Journal of Engineering Mechanics*, 126, 1232–1239.

Council of Standards Australia / NewZealand Standards Approval Board. (2018). *AS/NZS 2885.1:2018 Pipelines - Gas and liquid petroleum - Part 1: Design and construction*. Sydney, Australia.

Cugnetto, P., Robert, D., and Kajtaz, M. (2021). "Improved design guidelines for pipelines subjected to vertical fault movement in dry sand." *Journal of Pipeline Systems Engineering and Practice*, 12(4), 04021056.

D.G. Honegger Consulting SSD Inc. (2009). *Guidelines for constructing natural gas and liquid hydrocarbon pipelines through areas prone to landslide and subsidence hazards*. PRCI, Chantilly, VA, USA.

Daiyan, N., Kenny, S., Phillips, R., and Popescu, R. (2011). "Investigating pipeline-soil interaction under axial-lateral relative movements in sand." *Canadian Geotechnical Journal*, 48(11), 1683–1695.

Danciu, L., Hiemer, S., Nandan, S., Weatherill, G., Lammers, S., Rovida, A., Antonucci, A., Basili, R., Carafa, M. M. C., Kastelic, V., Maesano, F. E., Tiberti, M. M., Sesetyan, K., Vilanova, S., Beauval, C., Bard, P.-Y., Cotton, F., Wiemer, S., and Giardini, D. (2019). "Status, milestones and next activities on the development of the 2020 European Seismic Hazard Model (ESHM20)." *Geophysical Research Abstracts*, 21, 1.

Darigo, N., Rajah, S., and Boggess, L. (2008). "Preliminary surface fault assessment and conceptual fault crossing design of proposed gas pipeline, South-Central Alaska." *2008 7th International Pipeline Conference, Volume 3*, ASMEDC, 675–684.

Davis, C. A. (2008). "Assessing geotechnical hazards for water pipes with uniform confidence level." *Geotechnical Earthquake Engineering and Soil Dynamics IV*, ASCE, Reston, VA, 1–10.

Demirci, H. E., Bhattacharya, S., Karamitros, D. K., and Alexander, N. (2018). "Experimental and numerical modelling of buried pipelines crossing reverse faults." *Soil Dynamics and Earthquake Engineering*, 114, 198–214.

Dey, S., Chakraborty, S., and Tesfamariam, S. (2020). "Structural performance of buried pipeline undergoing strike-slip fault rupture in 3D using a non-linear sand model." *Soil Dynamics and Earthquake Engineering*, 135, 106180.

Dijkstra, G. J., Karamanos, S. A., Gresnigt, A. M., Sarvanis, G. C., and Dakoulas, P. (2021). "Actions due to severe ground-induced deformations." *Geohazards and pipelines*, S. A. Karamanos, A. M. Gresnigt, and G. J. Dijkstra, eds., Springer Nature Switzerland AG, Cham, Switzerland, 35–47.

Dilrukshi, S., and Wijewickreme, D. (2020). "Study of trench backfill particle size effects on lateral soil restraints on buried pipelines using discrete element modeling." *Journal of Pipeline Systems Engineering and Practice*, 11(1), 1–14.

Dorey, A. B., Murray, D. W., and Cheng, J. J. R. (2000). "An experimental evaluation of critical buckling strain criteria." *2000 Iternational Pipeline Conference*, ASME, Calgary, Alberta, Canada, 71–80.

European Committee for Standardization. (2004). *EN 1998-1:2004, Eurocode 8: Design of structures for earthquake resistance - Part 1: General rules, seismic actions and rules for buildings*. Brussels, Belgium.

European Committee for Standardization. (2006). *EN 1998-4:2006, Eurocode 8 - Design of structures for earthquake resistance - Part 4: Silos, tanks and pipelines*. CEN, Brussels, Belgium.

Fadaee, M., Farzaneganpour, F., and Anastasopoulos, I. (2020). "Response of buried pipeline subjected to reverse faulting." *Soil Dynamics and Earthquake Engineering*, 132, 106090.

Fragiadakis, M., Vamvatsikos, D., Karlaftis, M. G., Lagaros, N. D., and Papadrakakis, M. (2015). "Seismic assessment of structures and lifelines." *Journal of Sound and Vibration*, 334, 29–56.

Gantes, C. J., and Bouckovalas, G. D. (2013). "Seismic verification of the high pressure natural gas pipeline Komotini-Alexandroupoulis-Kipi in areas of active fault crossings." *Structural Engineering International: Journal of the International Association for Bridge and Structural Engineering (IABSE)*, 23(2), 204–208.

Gantes, C. J., and Melissianos, V. E. (2016). "Evaluation of seismic protection methods for buried fuel pipelines subjected to fault rupture." *Frontiers in Built Environment*, 2, 34.

Gawande, K., Kiran, R., and Cherukuri, H. P. (2019). "A numerical study of the response of buried steel pipelines undergoing strike-slip fault." *Engineering Failure Analysis*, 102, 203–218.

Giardini, D., Kauzar, S., and and the SERA Consortium. (2017). "EU H2020 SERA: Seismology and Earthquake Engineering Research Infrastructure Alliance for Europe." *19th European Geosciences Union General Assembly (EGU 2017)*, EGU, Vienna, Austria, EGU2017-14442.

Girgin, S., and Krausmann, E. (2016). “Historical analysis of U.S. onshore hazardous liquid pipeline accidents triggered by natural hazards.” *Journal of Loss Prevention in the Process Industries*, 40, 578–590.

Greiner, R., and Guggenberger, W. (1998). “Buckling behaviour of axially loaded steel cylinders on local supports - With and without internal pressure.” *Thin-Walled Structures*, 31(1–3), 159–167.

Gresnigt, A. M. (1986). “Plastic design of buried pipelines.” *HERON*, 31(4).

Ha, D., Abdoun, T. H., O’Rourke, M. J., Symans, M. D., O’Rourke, T. D., Palmer, M. C., and Stewart, H. E. (2010). “Earthquake faulting effects on buried pipelines - Case history and centrifuge study.” *Journal of Earthquake Engineering*, 14(5), 646–669.

Hamada, M., and O’Rourke, T. D. (1992). *Case studies of liquefaction and lifeline performance during past earthquakes*. *Technical Report NCEER-92-0001 NCEER*, Buffalo, NY, USA.

Hart, J. D., Lee, C., Kelson, K. I., and Hitchcock, C. (2004). “A unique pipeline fault crossing design for a highly focused fault.” *IPC2004 International Pipeline Conference*, ASCE, Calgary, Alberta, Canada.

Hasegawa, N., Nagamine, H., and Imai, T. (2014). “Development of "Steel Pipe for Crossing Fault (SPF)” using buckling pattern for water pipelines.” *JFE Technical Report*, 19, 61–65.

Honegger, D. G. (2017). *PRCI PR-268-134501-R01 Pipeline seismic design and assessment guideline*. Houston, TX, USA.

Honegger, D. G., Nyman, D. J., Johnson, E. R., Cluff, L. S., and Sorensen, S. P. (2004). “Trans-Alaska Pipeline System performance in the 2002 Denali fault, Alaska, earthquake.” *Earthquake Spectra*, 20(3), 707–738.

Houliara, S., and Karamanos, S. A. (2006). “Buckling and post-buckling of long pressurized elastic thin-walled tubes under in-plane bending.” *International Journal of Non-Linear*

Mechanics, 41(4), 491–511.
Indian Institute of Technology Kanpur. (2007). *IITK-GSDMA guidelines for seismic design of buried pipelines*. Kanpur, India.
International Organization for Standardization. (2019). *ISO 20074:2019 Petroleum and natural gas industry — Pipeline transportation systems — Geological hazard risk management for onshore pipeline*. Geneva, Switzerland.
Joshi, S., Prashant, A., Deb, A., and Jain, S. K. (2011). "Analysis of buried pipelines subjected to reverse fault motion." *Soil Dynamics and Earthquake Engineering*, 31(7), 930–940.
Jung, J. K., O'Rourke, T. D., and Argyrou, C. (2016). "Multi-directional force-displacement response of underground pipe in sand." *Canadian Geotechnical Journal*, 53(11), 1763–1781.
Jung, J. K., O'Rourke, T. D., and Olson, N. A. (2013a). "Uplift soil-pipe interaction in granular soil." *Canadian Geotechnical Journal*, 50(7), 744–753.
Jung, J. K., O'Rourke, T. D., Olson, N. A., O'Rourke, T. D., and Olson, N. A. (2013b). "Lateral soil-pipe interaction in dry and partially saturated sand." *Journal of Geotechnical and Geoenvironmental Engineering*, 139(12), 2028–2036.
Karamanos, S. A. (2002). "Bending instabilities of elastic tubes." *International Journal of Solids and Structures*, 39, 2059–2085.
Karamanos, S. A., Dijkstra, G. J., Sarvanis, G. C., Vazouras, P., Tsatsis, A., Van Es, S. H. J., Huinen, W., Dakoulas, P., Gazetas, G., Gresnigt, A. M., and Kourkoulis, R. (2021). "Numerical models for pipelines under large ground-inudced deformations." *Geohazards and pipelines*, S. A. Karamanos, A. M. Gresnigt, and G. J. Dijkstra, eds., Springer Nature Switzerland AG, Cham, Switzerland, 125–170.
Karamanos, S. A., Sarvanis, G. C., Keil, B. D., and Card, R. J. (2017). "Analysis and design of buried steel water pipelines in seismic areas." *Journal of Pipeline Systems Engineering*

and Practice, 8(4), 1–11.

Karamitros, D. K., Bouckovalas, G. D., and Kouretzis, G. P. (2007). “Stress analysis of buried steel pipelines at strike-slip fault crossings.” *Soil Dynamics and Earthquake Engineering*, 27(3), 200–211.

Karamitros, D. K., Bouckovalas, G. D., Kouretzis, G. P., and Gkesouli, V. (2011). “An analytical method for strength verification of buried steel pipelines at normal fault crossings.” *Soil Dynamics and Earthquake Engineering*, 31(11), 1452–1464.

Keaton, J. R., and Honegger, D. G. (2008). “Geotechnical challenges for design of a crude oil pipeline across an active normal fault in an urban area.” *2008 7th International Pipeline Conference, Volume 1*, ASME, 167–172.

Koch, T. (1933). “Analysis and effects of current movement on an active fault in Buena Vista Hills Oil Field, Kern County, California.” *AAPG Bulletin*, 17(6), 694–712.

Kouretzis, G. P., Bouckovalas, G. D., and Karamitros, D. K. (2011). “Seismic verification of long cylindrical underground structures considering Rayleigh wave effects.” *Tunnelling and Underground Space Technology*, 26(6), 789–794.

Kouretzis, G. P., Krabbenhøft, K., Sheng, D., and Sloan, S. W. (2014). “Soil-buried pipeline interaction for vertical downwards relative offset.” *Canadian Geotechnical Journal*, 51(10), 1087–1094.

Kouretzis, G. P., Sheng, D., and Sloan, S. W. (2013). “Sand-pipeline-trench lateral interaction effects for shallow buried pipelines.” *Computers and Geotechnics*, 54, 53–59.

Kouretzis, G., and Wu, J. (2021). “Recommendations for determining nonlinear Winkler spring parameters for buried steel pipe stress analysis applications.” *Computers and Geotechnics*, 135, 104196.

Kyriakides, S., and Corona, E. (2007). *Mechanics of offshore pipelines: Volume 1 Buckling and collapse*. Elsevier B.V., Oxford, UK.

Leonard, M. (2014). "Self-consistent earthquake fault-scaling relations: Update and extension to stable continental strike-slip faults." *Bulletin of the Seismological Society of America*, 104(6), 2953–2965.

Limam, A., Lee, L. H., Corona, E., and Kyriakides, S. (2010). "Inelastic wrinkling and collapse of tubes under combined bending and internal pressure." *International Journal of Mechanical Sciences*, 52(5), 637–647.

Liu, A., Hu, Y., Zhao, F., Li, X., Takada, S., and Zhao, L. (2004). "An equivalent-boundary method for the shell analysis of buried pipelines under fault movement." *Acta Seismologica Sinica*, 17(S1), 150–156.

Liu, B., Liu, X. J., and Zhang, H. (2009). "Strain-based design criteria of pipelines." *Journal of Loss Prevention in the Process Industries*, 22(6), 884–888.

Liu, M., Wang, Y.-Y., Song, Y., Horsley, D., and Nanney, S. (2012a). "Multi-tier tensile strain models for strain-based design Part 2 – Development and formulation of tensile strain capacity." *9th International Pipeline Conference*, ASME, Calgary, Alberta, Canada, IPC2012-90659.

Liu, M., Wang, Y., Horsley, D., Nanney, S., and Dot, U. S. (2012b). "Mutli-tier tensile strain models for strain-based design Part 3 – Model evaluation against experimental data." *9th International Pipeline Conference*, ASME, Calgary, Alberta, Canada, IPC2012-90660.

Liu, X., Zhang, H., Wu, K., Xia, M., Chen, Y., and Li, M. (2017). "Buckling failure mode analysis of buried X80 steel gas pipeline under reverse fault displacement." *Engineering Failure Analysis*, 77, 50–64.

Marino, G., and Osouli, A. (2020). "Slip resistance behavior of coal tar-coated steel pipelines buried in clayey and sandy Backfills from ground movement." *Journal of Pipeline Systems Engineering and Practice*, 11(3), 1–11.

Meidani, M., Meguid, M. A., and Chouinard, L. E. (2017). "Evaluation of soil–pipe interaction under relative axial ground movement." *Journal of Pipeline Systems Engineering and Practice*, 8(4), 04017009.

Melissianos, V. E., Danciu, L., Vamvatsikos, D., and Basili, R. (2021). "Fault displacement hazard estimation at lifeline-fault crossings: A baseline approach for engineering applications." *Earthquake Spectra*, under revision.

Melissianos, V. E., and Gantes, C. J. (2017). "Numerical modeling aspects of buried pipeline-fault crossing." *Computational Methods in Applied Sciences*, M. Papadrakakis, V. Plevris, and N. D. Lagaros, eds., Springer International Publishing, Cham, Switzerland, 1–26.

Melissianos, V. E., and Gantes, C. J. (2019). "Protection measures for buried steel pipelines subjected to fault rupture." *2nd International Conference on Natural Hazards & Infrastructure (ICONHIC2019)*, G. Gazetas and I. Anastasopoulos, eds., National Technical University of Athens, Chania, Greece.

Melissianos, V. E., Korakitis, G. P., Gantes, C. J., and Bouckovalas, G. D. (2016). "Numerical evaluation of the effectiveness of flexible joints in buried pipelines subjected to strike-slip fault rupture." *Soil Dynamics and Earthquake Engineering*, 90, 395–410.

Melissianos, V. E., Lignos, X. A., Bachas, K. K., and Gantes, C. J. (2017a). "Experimental investigation of pipes with flexible joints under fault rupture." *Journal of Constructional Steel Research*, 128, 633–648.

Melissianos, V. E., Vamvatsikos, D., and Gantes, C. J. (2017b). "Performance assessment of buried pipelines at fault crossings." *Earthquake Spectra*, 33(1), 201–218.

Melissianos, V. E., Vamvatsikos, D., and Gantes, C. J. (2017c). "Performance-based assessment of protection measures for buried pipes at strike-slip fault crossings." *Soil Dynamics and Earthquake Engineering*, 101, 1–11.

Melissianos, V. E., Vamvatsikos, D., and Gantes, C. J. (2020). "Methodology for failure mode prediction of onshore buried steel pipelines subjected to reverse fault rupture." *Soil*

Dynamics and Earthquake Engineering, 135, 106116.

Mohr, W. (2003). "Strain-based design of pipelines - Report project No. 45892GTH." *Project No. 45892GTH*, (45892), 137.

Mokhtari, M., and Alavi Nia, A. (2015). "The influence of using CFRP wraps on performance of buried steel pipelines under permanent ground deformations." *Soil Dynamics and Earthquake Engineering*, 73, 29–41.

Monroy-Concha, M., Wijewickreme, D., and Honegger, D. G. (2012). "Effectiveness of geotextile-lined pipeline trenches subjected to relative lateral seismic fault ground displacements." *15th World Conference on Earthquake Engineering*, Lisboa, Portugal.

Moradi, M., Rojhan, M., Galandarzadeh, A., and Takada, S. (2013). "Centrifuge modeling of buried continuous pipelines subjected to normal faulting." *Journal of Earthquake Engineering and Engineering Vibration*, 12(1), 155–164.

Nair, G. S., Dash, S. R., and Mondal, G. (2018). "Review of pipeline performance during earthquakes since 1906." *Journal of Performance of Constructed Facilities*, 32(6), 1–18.

Nair, G. S., Dash, S. R., and Mondal, G. (2019). *Effect of field bends on the response of buried pipelines crossing strike-slip fault*. *Lecture Notes in Civil Engineering*.

Nguyen, K. T., and Asimaki, D. (2018). "A modified uniaxial Bouc-Wen model for the simulation of transverse lateral pipe-cohesionless soil interaction." *Geotechnical Earthquake Engineering and Soil Dynamics V*, ASME, Austin, TX, USA, 25–35.

Ni, P., Mangalathu, S., and Liu, K. (2020). "Enhanced fragility analysis of buried pipelines through Lasso regression." *Acta Geotechnica*, 15(2), 471–487.

Ni, P., Qin, X., and Yi, Y. (2018). "Use of tire-derived aggregate for seismic mitigation of buried pipelines under strike-slip faults." *Soil Dynamics and Earthquake Engineering*, 115, 495–506.

Nyman, D. J., Lee, E. M., and Audibert, J. M. E. (2008). "Mitigating geohazards for international pipeline projects: Challenges and lessons learned.” *Proceedings of the Biennial International Pipeline Conference, IPC*, ASME, Calgary, Alberta, Canada, 3, 64405.

O’Rourke, M. J., and Liu, J. X. (2012). *Seismic design of buried and offshore pipelines. Monograph MCEER-12-MN04*. Multidisciplinary Center for Earthquake Engineering Research, Buffalo, NY, USA.

O’Rourke, T. D., Jung, J. K., and Argyrou, C. (2016). “Underground pipeline response to earthquake-induced ground deformation.” *Soil Dynamics and Earthquake Engineering*, 91, 272–283.

Ono, K., Yokota, Y., Sawada, Y., Kawabata, T., Ono, K., Yokota, Y., Sawada, Y., and Kawabata, T. (2017). “Lateral force-displacement prediction for buried pipe under different effective stress condition.” *International Journal of Geotechnical Engineering*.

Papadakis, G. A. (1999). “Major hazard pipelines: A comparative study of onshore transmission accidents.” *Journal of Loss Prevention in the Process Industries*, 12(1), 91–107.

Prion, H. G. L., and Birkemoe, P. C. (1992). “Beam-column behavior of fabricated steel tubular members.” *Journal of Structural Engineering*, 118(5), 1213–1232.

Qin, X., Ni, P., and Du, Y. J. (2019). “Buried rigid pipe-soil interaction in dense and medium sand backfills under downward relative movement: 2D finite element analysis.” *Transportation Geotechnics*, 21, 100286.

Rahman, M. A., and Taniyama, H. (2015). “Analysis of a buried pipeline subjected to fault displacement: A DEM and FEM study.” *Soil Dynamics and Earthquake Engineering*, 71, 49–62.

Rasouli, H., and Fatahi, B. (2020). “Geofoam blocks to protect buried pipelines subjected to strike-slip fault rupture.” *Geotextiles and Geomembranes*, 48(3), 257–274.

Robert, D. J. (2017). “A modified Mohr-Coulomb model to simulate the behavior of pipelines in unsaturated soils.” *Computers and Geotechnics*, 91, 146–160.

Robert, D. J., Britto, A., and Setunge, S. (2020). “Efficient approach to simulate soil–pipeline interaction.” *Journal of Pipeline Systems Engineering and Practice*, 11(1), 04019046.

Robert, D. J., Soga, K., O’Rourke, T. D., and Sakanoue, T. (2016). “Lateral load-displacement behavior of pipelines in unsaturated sands.” *Journal of Geotechnical and Geoenvironmental Engineering*, 142(11), 04016060.

Robert, D. J., and Thusyanthan, N. I. (2018). “Uplift resistance of buried pipelines in partially saturated sands.” *Computers and Geotechnics*, 97, 7–19.

Rofooei, F. R., Attari, N. K. A., and Jalali, H. H. (2018). “New method of modeling the behavior of buried steel distribution pipes subjected to reverse faulting.” *Journal of Pipeline Systems Engineering and Practice*, 9(1), 1–13.

Rojhani, M., Moradi, M., Galandarzadeh, A., and Takada, S. (2012). “Centrifuge modeling of buried continuous pipelines subjected to reverse faulting.” *Canadian Geotechnical Journal*, 49(6), 659–670.

Roy, K., Hawlader, B., Kenny, S., and Moore, I. (2016). “Finite element modeling of lateral pipeline-soil interactions in dense sand.” *Canadian Geotechnical Journal*, 53(3), 490–504.

Roy, K., Hawlader, B., Kenny, S., and Moore, I. (2018a). “Lateral resistance of pipes and strip anchors buried in dense sand.” *Canadian Geotechnical Journal*, 55(12), 1812–1823.

Roy, K., Hawlader, B., Kenny, S., and Moore, I. (2018b). “Upward pipe–soil interaction for shallowly buried pipelines in dense sand.” *Journal of Geotechnical and Geoenvironmental Engineering*, 144(11), 04018078.

Royal Netherlands Standardization Institute. (2020). *NEN 3650-1:2020 Requirements for pipeline systems - Part 1: General requirements*. Delft, The Netherlands.

Sarvanis, G. C., and Karamanos, S. A. (2017). “Analytical model for the strain analysis of continuous buried pipelines in geohazard areas.” *Engineering Structures*, 152, 57–69.

Sarvanis, G. C., Karamanos, S. A., Vazouras, P., Mecozzi, E., Lucci, A., and Dakoulas, P. (2018). “Permanent earthquake-induced actions in buried pipelines: Numerical modeling and experimental verification.” *Earthquake Engineering & Structural Dynamics*, 47(4), 966–987.

Sim, W. W., Towhata, I., Yamada, S., and Moinet, G. J. M. (2012). “Shaking table tests modelling small diameter pipes crossing a vertical fault.” *Soil Dynamics and Earthquake Engineering*, 35, 59–71.

Singhal, A. C. (1980). “Strength characteristics of buried jointed pipelines.” *Arizona State University Report Number ERC R80027, Grant #RC-A77-6A*, New York, NY, USA, 1–172.

Soveiti, S., and Mosalmani, R. (2020). “Mechanical behavior of buried composite pipelines subjected to strike-slip fault movement.” *Soil Dynamics and Earthquake Engineering*, 135, 106195.

Strogen, B., Bell, K., Breunig, H., and Zilberman, D. (2016). “Environmental, public health, and safety assessment of fuel pipelines and other freight transportation modes.” *Applied Energy*, 171, 266–276.

Strom, A., Ivaschenko, A., and Kozhurin, A. (2011). “Assessment of the design displacement values at seismic fault crossings and of their excess probability.” *Journal of Mountain Science*, 8(2), 228–233.

Tahamouli Roudsari, M., Hosseini, M., Ashrafy, M., Azin, M., Nasimi, M., Torkaman, M., and Khorsandi, A. (2019). “New method to evaluate the buried pipeline–sandy soil interaction subjected to strike slip faulting.” *Journal of Earthquake Engineering*.

Talebi, F., and Kiyono, J. (2020). “Introduction of the axial force terms to governing equation for buried pipeline subjected to strike-slip fault movements." *Soil Dynamics and Earthquake Engineering*, 133, 106125.

Thingbaijam, K. K. S., Mai, P. M., and Goda, K. (2017). "New empirical earthquake source-scaling laws." *Bulletin of the Seismological Society of America*, 107(5), 2225–2246.

Thompson, S., Madugo, C., Lewandowski, N., Lindvall, S., and Ketabdar, M. (2018). "Fault displacement hazard analysis methods and strategies for pipelines." *11th National National Conference in Earthquake Engineering*, EERI, Los Angeles, CA, USA.

Tian, Y., and Cassidy, M. J. (2011). "Pipe-soil interaction model incorporating large lateral displacements in calcareous sand." *Journal of Geotechnical and Geoenvironmental Engineering*, 137(3), 279–287.

Trautmann, C. H., and O'Rourke, T. D. (1983). "Behavior of pipe in dry sand under lateral and uplift loading." *Geotechnical Engineering Report 83-7*, Ithaca, NY, USA.

Trifonov, O. V. (2015). "Numerical stress-strain analysis of buried steel pipelines crossing active strike-slip faults with an emphasis on fault modeling aspects." *Journal of Pipeline Systems Engineering and Practice*, 6(1), 1–10.

Trifonov, O. V. (2018). "The effect of variation of soil conditions along the pipeline in the fault-crossing zone." *Soil Dynamics and Earthquake Engineering*, 104, 437–448.

Trifonov, O. V., and Cherniy, V. P. (2014). "Analysis of stress-strain state in a steel pipe strengthened with a composite wrap." *Journal of Pressure Vessel Technology, Transactions of the ASME*, 136(5), 1–8.

Trifonov, O. V., and Cherniy, V. P. (2016). "Application of composite wraps for strengthening of buried steel pipelines crossing active faults." *Journal of Pressure Vessel Technology, Transactions of the ASME*, 138(6), 2–3.

Tsai, C. C., Meymand, P., Dawson, E., and Wong, S. A. (2015). "Behaviour of segmental pipeline protective vaults subjected to fault offset." *Structure and Infrastructure*

Engineering, 11(10), 1369–1382.

Tsatsis, A., Loli, M., and Gazetas, G. (2019). “Pipeline in dense sand subjected to tectonic deformation from normal or reverse faulting.” *Soil Dynamics and Earthquake Engineering*, 127, 105780.

Tsinidis, G., Di Sarno, L., Sextos, A., and Furtner, P. (2020). “Optimal intensity measures for the structural assessment of buried steel natural gas pipelines due to seismically-induced axial compression at geotechnical discontinuities.” *Soil Dynamics and Earthquake Engineering*, 131, 106030.

Uckan, E., Akbas, B., Shen, J., Rou, W., Paolacci, F., and O’Rourke, M. J. (2015). “A simplified analysis model for determining the seismic response of buried steel pipes at strike-slip fault crossings.” *Soil Dynamics and Earthquake Engineering*, 75, 55–65.

United Kingdom Onshore Pipeline Operators’ Association. (2019). *Good practice guide - Seismic screening assessment of UK onshore pipelines and associated installations UKOPA/GP/019 Edition 1*. Derbyshire, UK.

United Nations. (2015). *Sendai Framework for Disaster Risk Reduction 2015 - 2030*. Geneva, Switzerland.

Valsamis, A. I., and Bouckovalas, G. D. (2020). “Analytical methodology for the verification of buried steel pipelines with flexible joints crossing strike-slip faults.” *Soil Dynamics and Earthquake Engineering*, 138, 106280.

Valsamis, A. I., Bouckovalas, G. D., and Gantes, C. J. (2020). “Alternative design of buried pipelines at active fault crossings using flexible joints.” *International Journal of Pressure Vessels and Piping*, 180, 104038.

Vasilikis, D., and Karamanos, S. A. (2011). “Buckling design of confined steel cylinders under external pressure.” *Journal of Pressure Vessel Technology, Transactions of the ASME*, 133(1), 1–9.

Vazouras, P., Dakoulas, P., and Karamanos, S. A. (2015). "Pipe-soil interaction and pipeline performance under strike-slip fault movements." *Soil Dynamics and Earthquake Engineering*, 72, 48–65.

Vazouras, P., and Karamanos, S. A. (2017). "Structural behavior of buried pipe bends and their effect on pipeline response in fault crossing areas." *Bulletin of Earthquake Engineering*, 15(11), 4999–5024.

Vazouras, P., Karamanos, S. A., and Dakoulas, P. (2010). "Finite element analysis of buried steel pipelines under strike-slip fault displacements." *Soil Dynamics and Earthquake Engineering*, 30(11), 1361–1376.

Wang, J. H. (2018). "A review on scaling of earthquake faults." *Terrestrial, Atmospheric and Oceanic Sciences*, 29(6), 589–610.

Wang, Y. (2019). *PRCI PR-350-164501-R01 Guidance for assessing buried pipelines after a ground movement event*. Houston, TX, USA.

Wang, Y., Cheng, W., and Horsley, D. (2004). "Tensile strain limits of buried defects in pipeline girth welds." *International Pipeline Conference*, Calgary, Alberta, Canada, IPC2004-524.

Wang, Y., Liu, M., Zhang, F., Horsley, D., and Nanney, S. (2012). "Multi-tier tensile strain models for strain-based design Part 1 - Fundamental basis." *9th International Pipeline Conference*, ASME, Calgary, Alberta, Canada, IPC2012-90690.

Wells, D. L., and Coppersmith, K. J. (1994). "New empirical relationships among magnitude, rupture length, rupture width, rupture area, and surface displacements." *Bulletin of the Seismological Society of America*, 84(4), 974–1002.

Wham, B. P., Berger, B. A., and O'Rourke, T. D. (2019). "Hazard-resistant steel pipeline response to large fault rupture." *Geo-Congress 2019*, ASCE, Philadelphia, PA, USA, GSP 308.

Wijewickreme, D., Karimian, H., and Honegger, D. (2009). “Response of buried steel pipelines subjected to relative axial soil movement.” *Canadian Geotechnical Journal*, 46(7), 735–752.

Wijewickreme, D., Monroy, M., Honegger, D. G., and Nyman, D. J. (2017). “Soil restraints on buried pipelines subjected to reverse-fault displacement.” *Canadian Geotechnical Journal*, 54(10), 1472–1481.

Wu, J., Kouretzis, G., and Suwal, L. (2020a). “Bearing capacity mechanisms for pipes buried in sand.” *Canadian Geotechnical Journal*, (July), 0–19.

Wu, J., Kouretzis, G., Suwal, L., Ansari, Y., and Sloan, S. W. (2020b). “Shallow and deep failure mechanisms during uplift and lateral dragging of buried pipes in sand.” *Canadian Geotechnical Journal*, 57(10), 1472–1483.

Xie, X., Symans, M. D., O’Rourke, M. J., Abdoun, T. H., O’Rourke, T. D., Palmer, M. C., and Stewart, H. E. (2013). “Numerical modeling of buried HDPE pipelines subjected to normal faulting: A case study.” *Earthquake Spectra*, 29(2), 609–632.

Xu, L., and Lin, M. (2017). “Analysis of buried pipelines subjected to reverse fault motion using the vector form intrinsic finite element method.” *Soil Dynamics and Earthquake Engineering*, 93, 61–83.

Xu, R., Jiang, R., and Qu, T. (2021). “Review of dynamic response of buried pipelines.” *Journal of Pipeline Systems Engineering and Practice*, 12(2), 03120003.

Youngs, R. R., Arabasz, W. J., Anderson, R. E., Ramelli, A. R., Ake, J. P., Slemmons, D. B., McCalpin, J. P., Doser, D. I., Fridrich, C. J., Swan, F. H., Rogers, A. M., Yount, J. C., Anderson, L. W., Smith, K. D., Bruhn, R. L., Knuepfer, P. L. K., Smith, R. B., DePolo, C. M., O’Leary, D. W., Coppersmith, K. J., Pezzopane, S. K., Schwartz, D. P., Whitney, J. W., Olig, S. S., and Toro, G. R. (2003). “A methodology for probabilistic fault displacement hazard analysis (PFDHA).” *Earthquake Spectra*, 19(1), 191–219.

Yun, H., and Kyriakides, S. (1990). “On the beam and shell modes of buckling of buried pipelines.” *Soil Dynamics and Earthquake Engineering*, 9(4), 179–193.

Zeng, X., Dong, F. fei, Xie, X. dong, and Du, G. feng. (2019). *A new analytical method of strain and deformation of pipeline under fault movement*. *International Journal of Pressure Vessels and Piping*.

Zhang, J., Liang, Z., Zhang, H., Feng, D., and Xia, C. (2016a). “Failure analysis of directional crossing pipeline and design of a protective device.” *Engineering Failure Analysis*, 66, 187–201.

Zhang, L., Zhao, X., Yan, X., and Yang, X. (2016b). “A new finite element model of buried steel pipelines crossing strike-slip faults considering equivalent boundary springs.” *Engineering Structures*, 123, 30–44.

Zhang, L., Zhao, X., Yan, X., and Yang, X. (2017). “Elastoplastic analysis of mechanical response of buried pipelines under strike-slip faults.” *International Journal of Geomechanics*, 17(4), 1–13.

Tables

Table 1. List of codes, standards, and guidelines for the design/assessment of buried pipelines at fault crossings.

Document	**Publisher**	**Country**
AS/NZS 2885.1:2018 Pipelines - Gas and liquid petroleum - Part 1: Design and construction	Council of Standards Australia / NewZealand Standards Approval Board (2018)	Australia / New Zealand
Z662:19 Oil and gas pipeline systems	Canadian Standards Association (2019)	Canada
EN 1998-4:2006 Eurocode 8 – Design of structures for earthquake resistance – Part 4: Silos, tanks and pipelines	European Committee for Standardization (2006)	European Union
IITK-GSDMA Guidelines for seismic design of buried pipelines	Indian Institute of Technology Kanpur (2007)	India
ISO 20074:2019 Petroleum and natural gas industry — Pipeline transportation systems — Geological hazard risk management for onshore pipeline	International Organization for Standardization (2019b)	International
NEN 3650-1 Requirements for pipeline systems – Part 1: General requirements	Royal Netherlands Standardization Institute (2020)	The Netherlands
Good Practice Guide Seismic screening assessment of UK onshore pipelines and associated installations	United Kingdom Onshore Pipeline Operators' Association (2019)	UK
ASCE Guidelines of the seismic design of oil and gas systems	American Society of Civil Engineers (1984)	USA
ALA Guidelines for the design of buried steel pipe	American Lifelines Alliance (2001)	USA
PRCI PR-268-134501-R01 Pipeline seismic design and assessment guideline	Pipeline Research Council International (Honegger 2017)	USA
ASME B31.8-2018 Guide for gas transmission and distribution piping systems	American Society of Mechanical Engineers (2018)	USA
PRCI PR-350-164501-R01 Guidance for assessing buried pipelines after a ground movement event	Pipeline Research Council International (Wang 2019)	USA

Table 2. Empirical fault scaling relations for $\Delta \sim f(L_F)$ for $L_F > 10\text{km}$ [Wells and Coppersmith (1994): WC1994, Leonard (2014): L2014, Thingbaijam et al. (2017): TMG2017].

Reference	**Expression for median value (Δ in m, L_F in km)**	**Expression parameters (α/β)**		
		normal	**reverse**	**strike-slip**
WC1994	$\log_{10}(\Delta) = \alpha + \beta \log_{10}(0.75L_F)$	-1.990 / 1.240	-0.600 / 0.310*	-1.700 / 1.040
L2014+ (INT)	$\log_{10}(\Delta_{sub}) = \alpha + \beta \log_{10}(1000L_F)$ $\Delta = \Delta_{sub}/1.32$	-3.799 / 0.833	-3.799 / 0.833	$10 \le L_F \le 40$ -3.844 / 0.833 $L_F > 40$ -2.310 / 0.500
L2014+ (SCR)	$\log_{10}(\Delta_{sub}) = \alpha + b \log_{10}(1000L_F)$ $\Delta = \Delta_{sub}/1.32$	-3.572 / 0.833	-3.572 / 0.833	$10 \le L_F \le 60$ -3.615 / 0.833 $L_F > 60$ -2.022 / 0.500
TMG2017	$\log_{10}(\Delta_{sub}) = \alpha + \beta \log_{10}(L_F)$ $\Delta = \Delta_{sub}/1.32$	-2.302 / 1.302	-1.456 / 0.975	-1.473 / 0.789

*WC1994 expressions for reverse fault mechanism are not significant at a 95% probability level

+Note on tectonic environment: Interplate (INT) refers to the plate boundaries, while Stable Continental Region (SCR) refers to midcontinental earthquakes.

Table 3. Beam-type and continuum numerical models for pipeline–fault crossings: Advantages and disadvantages.

Model aspects	**Model**	
	Beam-type	**Continuum**
Model detail	low	high
Development	easy	difficult
Requirement for experienced engineer	no	yes
Computing resources required	low	very high
Analysis time	a few minutes	a few hours
Potential significant convergence issues	no	yes
Appropriate for pipeline route with many bends	yes	no
Steel material modeling	detailed	detailed
Soil material modeling	simplified	very detailed
Trench geometry modeling	no	yes
Strain estimation	yes	yes
Cross-section ovalization (direct) assessment	no	yes
Local buckling and wrinkles (direct) assessment	no	yes

Table 4. Analytical approach to compute the trench size and shape effect in pipeline design after Chaloulos et al. (2017).

	Action
1	The ultimate soil pressure and displacement for both the natural ground (p_{ult}^{gr} and y_{ult}^{gr}) and backfill soil (without trench effects) are computed ($p_{ult,inf}^{bf}$ and $y_{ult,inf}^{bf}$) after code provisions.
2	If $p_{ult}^{gr} < p_{ult,inf}^{bf}$, then trench effects are omitted and natural ground properties are adopted for computing the lateral soil springs. If $p_{ult}^{gr} > p_{ult,inf}^{bf}$, then proceed to the following steps.
3	The minimum required horizontal ($x_{cr} = ax_{max}$) and vertical ($d_{cr} = D$) distances of the displaced pipeline are computed for ignoring the trench effects, where: $a = \begin{cases} 2.7 + 1.8\tanh[0.6(H/D - 8.5)]\text{, for loose backfill sand} \\ 1.5 + 0.6\tanh[0.6(H/D - 8.5)]\text{, for medium backfill sand} \end{cases}$ $\frac{x_{max}}{H} = 3.5e^{-0.27\left(\frac{H}{D}\right)}$ or $\frac{x_{max}}{D} = \begin{cases} 3.0 + 0.10(H/D)^{C_1} \text{ for } H/D > A \\ 13.1 - 1.2(H/D) \\ C_2 \text{ for } H/D > B \end{cases}$ with $C_1 = 1.9, C_2 = 1.1, A = 6.0, \text{and } B = 10.0 \text{ for loose sand } \gamma_{dry} = 14.8kN/m^3$ $C_1 = 2.4, C_2 = 1.7, A = 4.8, \text{and } B = 9.5 \text{ for medium sand } \gamma_{dry} = 16.4kN/m^3$.
4	If $d < d_{cr}$, then for limited trench depth, the correction factors $I_{d,p}$ and $I_{d,y}$ are: $\begin{cases} I_{d,p} = 1.1 \pm 0.1 \text{ and } I_{d,y} = 1.0 \text{ for loose sand and } H/D < 9.5 \\ I_{d,p} = 1.2 \pm 0.2 \text{ and } I_{d,y} = 1.2 \text{ for loose sand and } H/D \geq 9.5 \\ I_{d,p} = 1.0 \pm 0.1 \text{ and } I_{d,y} = 0.8 \text{ for medium sand and } H/D < 9.5 \\ I_{d,p} = 1.2 \pm 0.2 \text{ and } I_{d,y} = 1.0 \text{ for medium sand and } H/D \geq 9.5 \end{cases}$ If $d \geq d_{cr}$, then the correction factors are $I_{d,p} = I_{d,y} = 1.0$.
5	If $x < x_{cr}$, then for limited trench width, the correction factors $I_{w,p}$ and $I_{w,y}$ are: $I_{w,p} = (x/x_{cr})^{-I_{\theta,p}b_p} \geq 1.0$ and $I_{w,y} = (x/x_{cr})^{-I_{\theta,y}b_y} \geq 1.0$ with $b_p = 1.1 - 0.6\tanh[0.32(H/D - 3.2)]$ $I_{\theta,p} = 1 - 0.35\{1 - \tanh[0.32(H/D - 6.3)]\}\sqrt{\cos\theta}$ $b_y = \begin{cases} 0.55 - 0.55\tanh[0.42(H/D - 4.2)] \text{ for loose sand} \\ 0.70 - 0.70\tanh[0.35(H/D - 5.5)] \text{ for medium sand} \end{cases}$ $I_{\theta,y} = b_{y,\theta}/b_y = 1 + (I_{\theta,p} - 1)b_p/b_y$ If $x \geq x_{cr}$, then the correction factors are $I_{w,p} = I_{w,y} = 1.0$.
6	The ultimate soil pressure (p_{ult}^{bf}) and displacement (y_{ult}^{bf}) for considering trench effect in sand backfill are: $p_{ult}^{bf} = I_{d,p}I_{d,y}p_{ult,inf}^{bf}$ and $y_{ult}^{bf} = I_{w,p}I_{w,y}y_{ult,inf}^{bf}$. The pipeline analysis is performed using the minimum ultimate soil pressure and associated ultimate displacement of natural soil and backfill sand.

$$\text{Notations:}\begin{cases} D & \text{pipe diameter} \\ H & \text{burial depth} \\ \theta & \text{trench inclination} \end{cases}$$

Table 5. Determination of spring properties after Kouretzis and Wu (2021) for design application of buried steel pipelines embedded in sand backfill and subjected to fault rupture.

Spring	Peak reaction force
Lateral	$F_{lateral} = \left[\dfrac{1}{0.228\left(\frac{H}{D}\right) + 0.057}\right]\left[\gamma HDL \tan\varphi_{ps,p}\right]$ Validity: up to $\begin{cases} H/D = 7 \text{ to } 8 & \text{for loose to medium sand} \\ H/D = 13 \text{ to } 15 & \text{for dense sand} \end{cases}$
Upward	$F_{upward} = \left[\left(1 - \dfrac{\pi D}{8H}\right)\left(1.175 + 0.711\dfrac{H}{D}\right)\right]\left[\gamma HDL \tan\varphi_{ps,p}\right]$ Validity: up to $\begin{cases} H/D = 7 \text{ to } 8 & \text{for loose to medium sand} \\ H/D = 13 \text{ to } 15 & \text{for dense sand} \end{cases}$
Downward	$F_{downward} = +N_q\gamma HD + N_\gamma 0.5\gamma D^2$ with: $N_q = e^{\pi\tan\varphi^*}\left[\tan\left(45^\circ + \varphi^*/2\right)\right]^2$ for loose and dense sand $N_q = e^{3.8\varphi^*\tan\varphi^*}\left[\tan\left(45^\circ + \varphi^*/2\right)\right]^2$ for medium sand $N_\gamma = e^{0.18\varphi^* - 2.5}$ where: $\tan\varphi^* = \left(\dfrac{\cos\psi\cos\varphi_{ps,p}}{1 - \sin\psi\sin\varphi_{ps,p}}\right)\tan\varphi_{ps,p}$ Notation: γ : dry unit weight of sand H : embedment depth measured from the pipe springline D : pipe diameter L : pipe length $\varphi_{ps,p}$: peak plane strain friction angle, being correlated to the friction angle (φ_{ds}) measure from direct shear tests as $\tan\varphi_{ds} = \frac{\cos\psi\cos\varphi_{ps,p}}{1-\sin\psi\sin\varphi_{ps,p}}$ with $\psi = 1.25\left(\varphi_{ps,p} - \varphi_{crit}\right)$ being the dilation angle, and φ_{crit} is the critical state friction angle of sand
Spring	**Peak displacement**
Lateral	loose $0.112H/D + 0.139$ medium $0.085H/D + 0.087$ dense $0.035H/D + 0.026$
Upward	$0.01H$ to $0.02H$ for dense to loose sand $< 0.1D$
Downward	loose $0.1D$ medium $0.1D$ dense $0.2D$

Table 6. Preliminary selection criteria for pipe protection measures.

Category	**Criterion**
1. Design	1.1 Compatibility with fault mechanisms
	1.2 Compatibility with pipe–fault crossing geometry
	1.3 Compatibility with pipe cross-section geometry and steel grade
	1.4 Requirement for sophisticated analysis
	1.5 Requirement for experimental verification
	1.6 Compatibility with codes
2. Construction	2.1 Ease of on-site application
	2.2 Requirement for special installation equipment
	2.3 Special requirements for transportation to the construction site
3. Procurement	3.1 Availability in the market
	3.2 Production upon request
	3.3 High cost of purchase
	3.4 High cost of installation

Table 7. Illustrative examples of applying the preliminary selection criteria for pipe protection measures

Measure	**Design criteria**					
	1.1	1.2	1.3	1.4	1.5	1.6
Wall thickness increase	+	+	+	**x**	**x**	+
Pipe placement within culverts	x[+]	+	N/A	**x**	**x**	+
Backfilling with pumice	+	+	+	**x**	**x**	+
Introduction of flexible joints	+	+	N/A	+	+	**x**
Route changing with high radius	+	+	+	+	**x**	**x**
Measure	**Construction criteria**					
	2.1	2.2	2.3			
Wall thickness increase	+	**x**	**x**			
Pipe placement within culverts	+	+	+			
Backfilling with pumice	+	**x**	+			
Introduction of flexible joints	+	**x**	**x**			
Route changing with high radius	**x**	**x**	N/A			
Measure	**Procurement criteria**					
	3.1	3.2	3.3	3.4		
Wall thickness increase	+	**x**	**x**	**x**		
Pipe placement within culverts	+	+	+	+		
Backfilling with pumice	+	N/A	**x**	**x**		
Introduction of flexible joints	+	+	+	**x**		
Route changing with high radius	N/A	N/A	+	+		

Abbreviations: +: yes / compliance / required, **x**: no / not required, N/A: not applicable

[+] Compatible only with strike-slip fault mechanism

Table 8. Brief practical guidelines for the numerical modeling of protection measures.

Measure	**Category**	**FE model type**	**Modeling**
Steel grade upgrade	Pipe strengthening	Beam-type / Continuum	Modify steel material properties
Wall thickness increase		Beam-type / Continuum	Increase thickness of cross-section / Increase thickness of shell
Pipe wrapping		Continuum	Introduce a shell layer outside the pipe shell for the composite wrap, introduce appropriate contact between pipe and wrap
Trench backfilling with tire-derived aggregate	Soil friction reduction	Continuum	Model the entire soil block and the trench geometry, use material properties for the backfilling from experimental results
Use of geotextile-lined trenches		Continuum	Model the interfaces at trench walls
Trench backfilling with loose granular soil		Beam-type / Continuum	Modify soil properties (soil springs for the beam-type model and material law of 3D-solid elements for the continuum model)
Excavation of a wider trench		Continuum	Model trench geometry
Pipe placing within culverts		Beam-type / Continuum	Do not model soil (remove soil springs / 3D-solid elements) along
Replace soil backfill with EPS geofoam blocks		Continuum	Model trench geometry and backfill materials with detail
Device applying external pressure	Complex measures	Continuum	Model after Zhang et al. (2016)
Pipe route change		Beam-type	Model the entire pipe route
Introduction of flexible joints		Beam-type	Model joints with springs (Melissianos et al. 2016; Valsamis and Bouckovalas 2020)
Pipeline offset at the crossing		Beam-type	Model with detail the entire pipe route (Hart et al. 2004)
Use field bends		Beam-type and continuum	Model the entire pipe route and assess the integrity of bends with detailed modeling (Vazouras and Karamanos 2017)
Pipe with predefined buckling pattern		Continuum	Model with detail the pipe shell (Hasegawa et al. 2014)